

MASTER THESIS



**ENHANCING UPPER LIMB PROSTHETICS  
DESIGN FOR IMPROVED STRENGTH  
AND MODULARITY: AN USER-FOCUSED  
APPROACH IN SIERRA LEONE**

Dennis Oonk  
s2633876

FACULTY OF ENGINEERING TECHNOLOGY  
DEPARTMENT OF BIOMECHANICAL ENGINEERING

**EXAMINATION COMMITTEE**

prof. dr. ir. Gabriëlle J.M. Tuijthof  
dr. ir. Izad Tamadon  
dr. Ali Sadeghi  
Merel van der Stelt

**DOCUMENT NUMBER**  
BE - 964

## Title page

Report:	Master Thesis Report
External Faculty:	Radboudumc, 3D Sierra Leone Project <a href="https://www.3dsierraleone.com/">https://www.3dsierraleone.com/</a>
Address:	Geert Groteplein Noord 15 Nijmegen 6525 EZ Netherlands
<b>General Supervisor Radboudumc</b>	
Faculty Supervisor:	Merel van der Stelt
Function:	Project Manager, PhD-candidate
E-Mail:	<a href="mailto:merel.vanderstelt@radboudumc.nl">merel.vanderstelt@radboudumc.nl</a>
Phone:	+31 6 28 55 03 74
Academic Institute:	University of Twente
Study:	Biomedical Engineering
<b>Chairman University of Twente</b>	
Faculty of Engineering Technology:	Gabriëlle J.M. Tuijthof
Function:	Full Professor
E-mail:	<a href="mailto:g.j.m.tuijthof@utwente.nl">g.j.m.tuijthof@utwente.nl</a>
Phone:	+31 5 34 89 93 22
<b>Technical Supervisor University of Twente</b>	
Faculty of Engineering Technology:	Izad Tamadon
Function:	Assistant Professor
E-mail:	<a href="mailto:i.tamadon@utwente.nl">i.tamadon@utwente.nl</a>
Phone:	+31 5 34 89 29 34
<b>Supervisor University of Twente</b>	
Faculty of Engineering Technology:	Ali Sadeghi
Function:	Assistant Professor
E-mail:	<a href="mailto:a.sadeghi@utwente.nl">a.sadeghi@utwente.nl</a>
Phone:	+31 5 34 89 90 66
<b>Student University of Twente</b>	
Student:	Dennis Oonk
Student number:	2633876
E-mail:	<a href="mailto:d.oonk-1@student.utwente.nl">d.oonk-1@student.utwente.nl</a>
Phone:	+31 6 34 85 55 95

## Abstract

*Introduction:* The application of 3D printing technology has experienced remarkable growth and offers new opportunities for improving upper limb prosthetics, particularly in resource-constrained countries. This study investigates the development and optimization of 3D-printed upper limb prostheses tailored to the unique challenges in third-world countries.

*Aim:* Our goal is to design, evaluate and optimize upper limb prosthetic connections for superior modularity, taking into account strength.

*Methods:* A modular design approach is used, combined with Finite Element Analysis (FEA) and physical testing, to evaluate various concepts. An iterative design approach is applied to ensure improvements in the concepts.

*Results:* The iterative design approach resulted in a combined solution between the strengths of two concepts with superior mechanical strength and improved modularity combined with a higher user-friendly operating approach. The FEA analysis proved the final design in keeping the required force and it demonstrated the breaking point correctly.

*Conclusion:* The fusion of innovative 3D printing technologies and modular design concepts offers a customizable approach, with significant potential for patients in resource-limited settings. A design methodology reaches to a final concept for modular 3D printed connections in upper limb prosthetics. Further testing with patient feedback is recommended to improve usability.

*Keywords:* Prosthesis 3D printing, finite element analysis, modular mechanical design, upper limb prosthesis.

# Table of Contents

<b>Title page</b> .....	2
<b>Abstract</b> .....	3
<b>1. Introduction</b> .....	6
1.1. General background .....	6
1.2. Specific Focus .....	7
<b>2. Methods</b> .....	11
2.1. Production Process and Material Selection .....	11
2.1.1. Production Process.....	11
2.1.2. Chosen material.....	12
2.2. Design Process and Selection .....	12
2.2.1. Program of Requirements .....	13
2.2.2. Concept Generation .....	14
2.2.3. Criteria .....	15
2.2.4. Final concept selection .....	17
2.3. Testing Procedures .....	18
2.3.1. FEA Simulations .....	18
2.3.2. Physical Testing .....	19
<b>3. Results</b> .....	21
3.1. Concept Illustration .....	21
3.1.1. Initial Strength Exploration Forearm of the Concepts .....	22
3.1.2. Concept Selection.....	23
3.1.3. Concept Selection.....	23
3.2. Iterative Development .....	24
3.2.1. Threaded connections.....	24
3.2.2. Wrist Adaptation .....	26
3.3. Glued Connections .....	28
3.4. Final Concept.....	28
3.5. Concept Score.....	30
<b>4. Discussion</b> .....	31
<b>5. Conclusion</b> .....	34
<b>References</b> .....	35
<b>Appendix</b> .....	38
Appendix A: Program of Requirements.....	38
Appendix B: Morphological Overview Selected .....	39
Appendix C: FEA for the Concepts.....	40

Appendix D: Scoring Tables .....	46
Appendix E: Iterative Steps .....	47
Appendix E.1. Iterative Steps - Threaded Concept.....	47
Appendix E.2. Iterative Steps - Omega Concept.....	49
Appendix F: Proof of Concepts .....	53
Appendix F.1. Proof of Concepts - Threaded Concept .....	53
Appendix F.2. Proof of Concepts - Omega Concept.....	55
Appendix G: Additional FEA.....	57
Appendix G.1. Additional FEA - Threaded Concept.....	57
Appendix G.2. Additional FEA - Omega Concept.....	60
Appendix H: Final Scoring Tables .....	63
Appendix I: FEA Simplified Wrist Adapter .....	64

# 1. Introduction

## 1.1. General background

The application of 3D printing technology has boomed in recent years and has brought about transformative changes in several areas, particularly prosthetics. The impact of 3D printing on prosthetics goes beyond cost-effectiveness and accessibility. This innovation has opened new horizons for the development and adaptation of prosthetic devices. Prosthetics fabricated using 3D printing technology have the potential to significantly improve the quality of life for people with limb loss, allowing them to regain their lost functionality and actively participate in daily routines and physical activities that might otherwise have been challenging [1]. One of the key advantages of 3D printing is its adaptability to diverse socioeconomic environments, making it a versatile choice for both resource-limited and affluent regions [2].

Moreover, the dynamic nature of 3D printing continues to drive progress in the prosthetic world. Innovations in materials and designs are constantly emerging to maximize the comfort, functionality and aesthetic appeal of 3D-printed prosthetics. The malleability and precision enabled by 3D printing technologies allow designers to customize prosthetics in ways previously unattainable, pushing the boundaries of what is possible

Provision of prosthetic care in low- and middle-income countries faces a host of challenges. The provision of prosthetic care is hampered by a range of economic, infrastructural, and sociocultural factors, which often result in limited access to quality prosthetics. These challenges stem primarily from [1]–[6]:

- **Economic constraints:** Limited financial resources and access to adequate healthcare infrastructure contribute to the scarcity of prosthetic supplies in many developing regions. The cost of traditional prosthetic devices may be prohibitive for both individuals and healthcare systems. The cost of traditional prostheses can be unaffordable for both individuals and healthcare systems, hindering widespread access to these essential medical devices.
- **Technological limitations:** Insufficient access to advanced prosthetic technologies in low-care areas hinders the development and distribution of advanced, customized prosthetic devices. This leads to over-reliance on outdated designs that may not be suitable for people's specific needs.
- **Geographic isolation:** Remote and rural areas often lack healthcare infrastructure. The lack of prosthetic clinics and trained professionals in these regions only compounds the challenges for people who need prosthetic care.
- **Lack of skilled personnel:** A shortage of skilled prosthetists and orthotists in many third-world countries limits the provision of proper clinical assessments and fitting services. This scarcity of skilled personnel leads to suboptimal fitting and placement of prostheses.
- **Social stigma and awareness:** Negative perceptions of disability and lack of awareness about the benefits of prostheses contribute to people's reluctance to seek prosthetic care. Social stigma and associated psychological barriers may further limit access to prosthetic solutions.
- **Environmental challenges:** Challenging environmental conditions in some regions, such as harsh climates and uneven terrain, require robust and adaptable prosthetic designs. Traditional prosthetic components may not be suitable for such conditions, leading to reduced durability and functionality.

- **Accessibility of materials and components:** A shortage of high-quality materials and components essential for prosthesis manufacturing hinders local production. Dependence on imported materials increases costs and may lead to further delays in care.

One of the third-world countries is Sierra Leone, which is located in West Africa. Sierra Leone has been affected by several wars and epidemics, including the Ebola virus outbreak, which has resulted in a high number of amputations. According to the World Health Organization (WHO), the prevalence of disability in low- and mid-income countries is estimated to be 10%, and a significant proportion of these disabilities are caused by amputations [7]. The high rates of amputations in Sierra Leone have created a need for affordable and accessible prosthetic devices. However, the cost of conventional prosthetic devices is often too high for many individuals in Sierra Leone, and access to such devices is limited [8].

To tackle this problem, the 3D Sierra Leone project (3DSL) was funded in 2018. This project is a collaboration between the Radboudumc and local partners of the Masanga Hospital in Sierra Leone, aimed at using 3D technologies to improve healthcare in the region. The project focuses on developing customized 3D-printed prosthetics and orthotics for amputees and individuals with disabilities. Additionally, the project involves training local healthcare workers on the use of these 3D technologies, thereby increasing their capacity to provide better care for their patients.

The selection of Masanga Hospital was deliberate for several key reasons. Firstly, the hospital houses a substantial research department overseen by Professor M. Grobusch, affiliated with the Center of Tropical Medicine and Travel Medicine at Amsterdam University Medical Center in The Netherlands. Furthermore, Masanga Hospital has gained recognition for its expertise in wound care, with a notable volume of amputation procedures being conducted within its facilities [8].

The 3DSL project mainly provides prosthetics for four types of amputation: 1. Transtibial, 2. Transfemoral, 3. Transradial and 4. Transhumeral. This project will focus on the transradial and transhumeral prosthetic devices and these types of prostheses will be referred to as upper limb prostheses further in this report.

The first designed upper limb prostheses provided by the 3D Sierra Leone project were created without any standard available design guidelines, it was performed by trial and error using scans of the residual limb and contralateral arm [9], [10]. This process was time-consuming and required a significant amount of knowledge and expertise which was not available from the local staff of Masanga Hospital because of the limited computer experience [10]. Despite these challenges, the 3D Sierra Leone project has been successful in providing upper limb prostheses to Sierra Leoneans with limb amputations. These prostheses have helped improve the quality of life for individuals who have lost a limb, allowing them to perform daily activities and participate in their communities [11]. Hereafter, prosthetics were created using a standard workflow. This allowed for the prosthetics to be made faster. However, the local people could not make the design independent yet. To overcome this problem and the required knowledge and expertise needed for the upper limb prostheses, the 3DSL project had the demand for an automated digital design process for sockets and standardized manufacturing of 3D-printed prostheses utilizing self-made software [10].

## 1.2. Specific Focus

As mentioned before, this project focuses on upper limb prostheses which consist of transradial and transhumeral prosthetic devices. The connection methods for the transradial prosthetic are located in the triceps plate to the forearm and in the forearm to the hand, see Figure 1. For transhumeral prosthetics, the most common connection methods are located in the socket to the elbow, in the

elbow to the forearm and in the forearm to the hand, see Figure 3. The connection methods in the wrist and above/below the elbow module are currently fixated using glue. The most common disadvantage of this technique is that the connection is based on adhesive bonding and the entire prosthetic device must be reprinted if one compartment breaks. Another disadvantage is that the hand cannot be reoriented or swapped with another device. For these reasons, the project aims is to improve the modularity of the connection methods above and below the elbow module in the case of the transhumeral prosthetic device, and in the wrist joint of the adjustable 3D-printed upper limb prosthetic devices for upper limb amputees in Sierra Leone, while maintaining the requested strength.

### Transradial and connections

Besides the transhumeral prosthesis, the 3DSL project also contains a design for the transradial prosthesis, see Figure 1. This design uses the same hand model as the transhumeral prosthetic device. The socket is applied on the forearm which is connected to a plate located on the Triceps (the Triceps plate) using two hinge plates located near the medial and lateral epicondyles [13], the yellow arrows in Figure 1 indicate where the hinge plates are connected to the transradial prosthesis and Triceps plate on the medial side, this is at the same location on the lateral side.

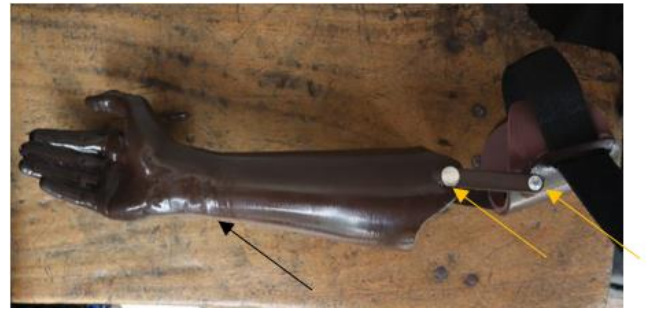


Figure 1 Full-size Transradial model where the connection points of the hinge plates are pointed to the medial side by the yellow arrows. The black arrow points to the glued and soldered connection area between the hand and arm.

The black arrow points to the area where the hand is connected to the forearm. The connection is not only glued but also soldered as mentioned before. This increases the strength of the connection but also limits modularity.

As mentioned before, the Triceps plate is connected to the transradial socket by hinge plates. These plates are designed with a bending in the middle, see Figure 2. These bending parts should prevent interference with the elbow joint as the Triceps plate is smaller compared to the width of the transhumeral socket where the hinge plates connect. The ends of the hinge plate should be straight as the flat areas ensure a good alignment with the pivot axes.

An extra smaller plate could be added when an additional pivot point is desired as shown by the yellow arrow in Figure 2. While this hinge plate is mentioned in this section, the connection to the transradial socket will not be covered in this project as the focus is only on the connections in the wrist (transradial and transhumeral) and above/ below elbow module (transhumeral).



Figure 2 Triceps plate with hinge plate and an extra smaller plate for an additional pivot point

### Transhumeral and connections

The socket above the elbow is created using a 3D scan of the stump of the patient [12]. The elbow module is designed by a previous student to allow for flexion and extension in the transhumeral prosthetic device [9], see Figure 3. This elbow consists of 2 sizes, 70 mm and 90 mm in diameter, to fit the bayonet connector of the socket.

The elbow module contains two different methods for connecting the elbow to the socket and the forearm. As mentioned, the connection with the socket is accomplished using a bayonet connection (black arrow). The socket is placed on these points where the connection areas are glued together.



This method allows for strain relief through the bayonet connection where the forces are applied [9]. The connection method allows for a slight change in rotation of the elbow module compared to the socket when desired. The adhesive bonding of the glue also prevents the socket to continue rotating and falling off from the elbow, however, this bonding is not optimal [9].

The extending circumference part of the bottom of the elbow module will be glued to the forearm (blue arrow). As a result, the strength in connection of the forearm with the elbow is based on the adhesive bonding of the glue alone. The grooves in this part act as a guidance for the lower arm for the correct positioning.

The forearm is designed in two different sizes as well to fit the 70 mm and 90 mm diameter of the elbow module.

The forearm can then be scaled in the Z-axis to match the length of the contralateral forearm.

The hand model consists of a pre-scanned hand which is scaled to different sizes to match the contralateral hand: extra small, small, medium, and large. The hand can fit together with the forearm using a lip and groove method. This is then glued together as indicated by the brown arrow in Figure 3.



*Figure 3 Transhumeral prosthetic device design. The black arrow highlights the bayonet connection above the elbow module; the blue arrow highlights the glued connection to the forearm; the brown arrow highlights the glued connection to the wrist.*

The use of adhesive bonding, to connect various modules in the upper limb prosthesis, can pose challenges related to the strength and modularity of the device. While adhesive bonding can provide a strong connection, the axial strength of the device heavily relies on the quality of the bond. According to O. Kamara (personal communication, April 18, 2023) who makes the prosthetic devices at Masanga Hospital, the connection method in the wrist has been broken by one patient before in the axial direction, and this was then solved by melting the transition edges of the hand and forearm together using a soldering iron. Since then, the prosthetic device has not broken down.

### **3D Model**

Figure 4 illustrates the 3D model of the Transhumeral prosthetic device including the hand and the socket which will be attached to the stump of the patient. The hand and the socket are removed in the picture in the exploded view in the middle. Next, on the right in the figure is the cross-section of the elbow module, forearm and the wrist connection attached. As mentioned before, the connection methods which will be investigated are located above and below the elbow module as well as in the adapter in the wrist, as highlighted by the yellow boxes. These locations in the cross sections are also used in the method to generate different concepts in subchapter 2.2. Design Process and Selection.

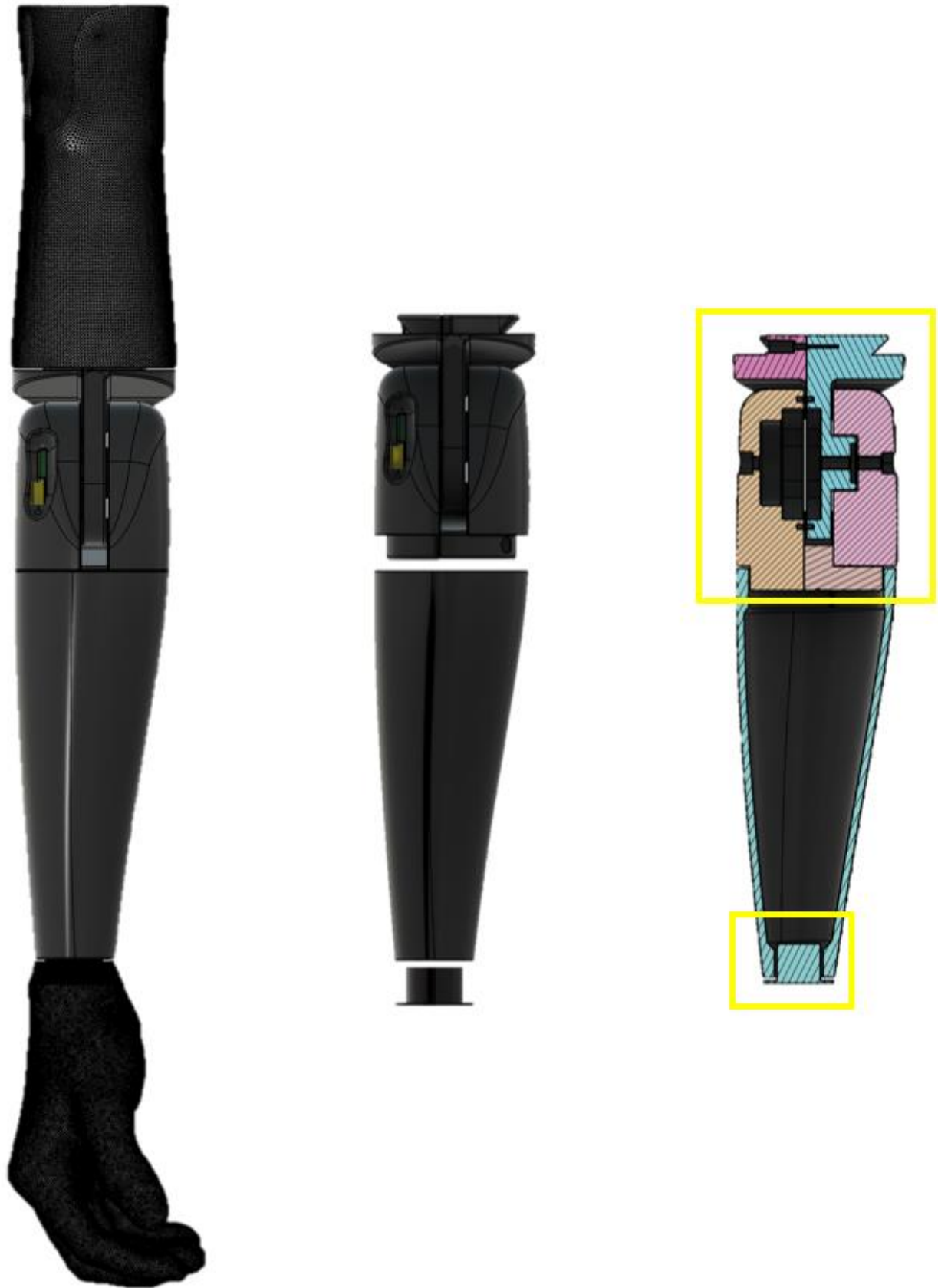


Figure 4 3D Model of the transhumeral prosthetic currently applied in Sierra Leone.  
 Left: Full overview of the arm including the hand and the socket for the stump.  
 Middle: Exploded view of the elbow module, the forearm and the adapter of the hand.  
 Right: Cross section of the elbow module, forearm and adapter in the wrist. The yellow boxes indicate the cross sections of the connection methods (above/ below elbow module and the wrist). This visualisation will be used in the generation of concepts.

## 2. Methods

### 2.1. Production Process and Material Selection

The production process and material selection for upper limb prosthetic connections are pivotal components, influencing both the durability and functionality of the end product. This section delves into the critical considerations that guide the established production process and material selection.

#### 2.1.1. Production Process

The selection of Fused Deposition Modeling (FDM) as the 3D printing production process for prosthetic devices is underpinned by several key advantages. FDM excels in the fabrication of patient-specific components, ensuring an exquisite fit for each amputee [19]. The combination of 3D scanning and FDM technology optimizes the production pipeline, reduces potential errors and speeds up delivery. The inherent ability of FDM to create intricate geometries is well-suited to the versatile mechanical requirements of prosthetic connections, thereby enabling adaptability. Furthermore, its iterative prototyping capabilities streamline design refinements, minimizing development time [5].

In contrast, the utilization of conventional manufacturing methods, such as casting, relies on rigid moulds and templates. These components exhibit limited adaptability to meet the specific requirements of individual patients. Consequently, the creation of bespoke moulds for each patient becomes a financially burdensome and time-intensive endeavour. In the case of machining, although it boasts remarkable precision, the complexity and associated expenses entailed in crafting customized components for every patient render it less practicable for widespread implementation.

Moreover, the decision to employ Fused Deposition Modelling (FDM) as the production process brings an additional benefit – the pre-existing presence of Ultimaker 3D printers within the 3D Lab at Masanga Hospital. Opting for an alternative production approach for arm prosthetics would necessitate the acquisition of new machinery, amplifying costs in contrast to the use of FDM, which synergizes seamlessly with the existing infrastructure, further underscoring its cost-efficiency. Consequently, FDM is chosen not only for its patient-specific and adaptable attributes but also for its economic feasibility due to a reduction in personnel and manufacturing costs [20]–[23].

Optimizing the mechanical strength of FDM-printed sockets is vital to address drawbacks, such as reduced load-bearing capacity and material toughness in the perpendicular print direction, which stem from the reduced bonding area between layers [24]. This limitation can lead to potential failures due to stress concentration at inter-layer notches [25], [26].

To enhance mechanical strength under both static and fatigue loading, it's crucial to consider specific parameters during both the printing process and design of AM PLA for prosthetic connections [27], [28]:

- layer thickness,
- infill percentage,
- nozzle size,
- manufacturing orientation,
- filling pattern,
- filling rate,
- feed rate,
- manufacturing rate,
- shell thickness (set equal to a multiple of the nozzle diameter),
- and filling temperature.

In terms of engineering static assessment, much experimental evidence suggests that the effect of these parameters on the elastic modulus, yield stress and the ultimate tensile strength can be neglected with little loss of accuracy. This means that, for design and FEA simulation purposes, AM PLA can be treated simply as a homogenous, isotropic, and linear-elastic material [29].

### 2.1.2. Chosen material

In the design process, material selection holds paramount importance. The chosen material should possess a trifecta of qualities: strength, durability, and lightness, while simultaneously being biocompatible to avert adverse reactions or skin irritation [17]. To make a judicious selection, it is imperative to consider the intended use of the prosthetic device and the requisite mechanical properties for its proper functioning [18]. Additionally, in resource-constrained environments, the local availability and affordability of materials become pivotal factors in the design-making process [19].

A comprehensive study by Merel v.d. Stelt et al. [8] has firmly established Tough Polylactic Acid (Tough PLA) as an optimal material choice, nearly aligning with the ISO-10328 standards for testing lower limb prosthetic devices. The mechanical properties of Tough PLA closely align with the project's requirements and design considerations, ensuring exceptional performance and reliability when produced using FDM. Additionally, the ease of printing and proven performance in lower leg prosthetics further underscore the suitability of Tough PLA for this application.

The following properties highlight the suitability of Tough PLA for the transversal direction:

- **Tensile Strength (MPa):**  
This property signifies the material's ability to withstand axial forces and resist deformation under tension. Tough PLA exhibits a tensile strength of 27.9 MPa.
- **Tensile Modulus (MPa):**  
This property is critical for maintaining the structural integrity of the connection methods, especially when subjected to bending or torsional forces. The tensile modulus of Tough PLA is 1316.7 MPa.
- **Tensile Elongation at Break (%):**  
This property ensures that the material can undergo some deformation before reaching its breaking point, contributing to the safety and durability of the prosthetic connections. Tough PLA provides a tensile elongation at a break of 3.7%.
- **Yield Strength (MPa):**  
This property represents the point at which the material begins to deform plastically under stress. A well-defined yield point is valuable for understanding the material's behaviour under load, aiding in design considerations. Tough PLA contains a yield strength of 20 MPa. This value is used during the FEA of the concepts to function as a limit for the maximum stresses.

## 2.2. Design Process and Selection

For the design process of connection methods in 3D-printed upper limb prosthetics, a sequence of phases will be followed, by employing the method established by Zeiler [14]. In the pursuit of arriving at a definitive concept, the process is initiated by creating a comprehensive program of requirements. Subsequently, this program was transformed into functional elements from which the functions could be executed through various methods. By choosing distinct operational modes for each function, a range of concepts were generated. The ultimate concept was ultimately selected

through an evaluation of these generated ideas, based on the predetermined criteria of the program of requirements.

### 2.2.1. Program of Requirements

The design process of 3D-printed upper limb prostheses in middle and low-income countries such as Sierra Leone must consider several requirements to meet user needs while being affordable and culturally appropriate. It is crucial to design 3D-printed prosthetic devices that can be easily customized and modified to meet the user's changing needs. To ensure this, a meticulous analysis of the Program of Requirements (POR) was conducted. This POR is a comprehensive document that is derived from the needs of both the 3DSL project at Radboudumc and the Masanga Hospital staff. Several requirements are:

#### **Mechanical Integrity**

Ensuring the mechanical integrity of the connection methods is paramount. These prosthetic devices need to withstand the stresses of daily activities. This involves extensive mechanical testing, such as tensile strength analysis, stress simulations, and yield strength assessments [15].

#### **Functionality**

Despite the project's primary focus on a passive prosthesis, devoid of additional functionalities, it remains crucial to infuse functionality through the adjustability and replacement of the wrist module. This augmentation allows the hand to be positioned in various ways, empowering the patient to adapt to diverse situations [16].

#### **Cost-Effectiveness and Accessibility**

The design must be financially viable, especially in resource-constrained settings. Each element should be optimized for production efficiency, cost-effectiveness, and ease of maintenance, helping ensure accessibility for the target user population [17].

#### **Durability and Longevity**

Long-term durability is a hallmark of a successful prosthetic connection. The materials used must resist wear and tear, and the connections should maintain their performance over time. Analysis of product lifetimes and failure rates is essential for data-driven design improvements, making it possible to create connections that maintain their performance and longevity, even in challenging environments [18].

Within the POR, the requirements are categorized into functional and fabrication aspects. To ascertain the definitive nature of each requirement, whether fixed or variable, discussions are held with the Masanga Hospital personnel. The ultimate concept selection depends on the variable requirements, as each conceptual iteration is evaluated based on these criteria. To facilitate this decision-making process, the Kesselring methodology is applied, with specific weights assigned to prioritize variable requirements. Table 2 presents the weights associated with variable requirements codes and a detailed breakdown of these codes and their corresponding full descriptions. These weights are determined through extensive consultations with Masanga Hospital personnel, emphasizing the importance of certain requirements by assigning higher weights to them. The POR, in its entirety, is provided in Appendix A for reference.

Table 1 Weights of variable Requirements and the corresponding description of the codes

Selected requirement	Compared to						Total	Weight
	Fu - As 2	Fu - As 3	Fa - Co 1	Fa - Re 2	Fa - We 1	Fa - We 2		
Fu - As 2	x	0	1	0	1	1	3	3
Fu - As 3	1	x	1	1	1	1	5	4
Fa - Co 1	0	0	x	0	0	1	1	2
Fa - Re 2	1	0	1	x	1	1	4	3
Fa - We 1	0	0	1	0	x	1	2	2
Fa - We 2	0	0	0	0	0	x	0	1

Requirement Code	Requirement Type	Requirement Description
Fu – As 2	Functional - Assembly	The prosthetic device allows the patient to assemble the prosthetic device in less than 10 steps
Fu – As 3	Functional - Assembly	The connection methods allow for one-handed assembly.
Fa – Co 1	Fabrication – Costs	The connection methods are designed with cost-effectiveness in mind to keep the costs of the prosthetic devices below 30 euros
Fa – Re 2	Fabrication - Realization	The prosthetic device is compatible with 3D printing technology
Fa – We 1	Fabrication - Weight	The weight of the prosthetic device with the connection methods does not exceed 1,5 kg
Fa – We 2	Fabrication - Weight	The positioning of the hand minimizes the need for support structures during the printing process



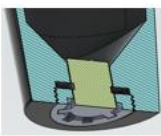


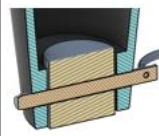







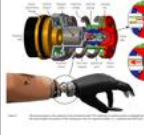






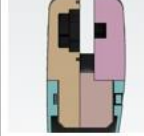



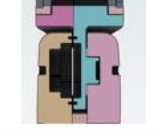



### 2.2.2. Concept Generation

The various concepts are generated using a design method known as a morphological overview. With this method, the different functions that the concept should accommodate are placed in a column in the table. As the prosthetic device is a passive prosthetic device, actuations are not applicable, which reduces the overall functions to five functions for transhumeral prosthetic devices. For transradial prosthetic devices, only the functions in the wrist are of interest.

Using different brainstorming sessions, various methods to realize these functions are placed per function in the columns on the right in the morphological overview table. These methods are visually represented using a picture. By selecting different methods for each function, various concepts are created. These diverse methods were intuitively chosen, considering which options seemed most promising, and served as the foundation for further logical connections. The aim is to develop a range of concepts that comprehensively address arm functions in the most effective and user-friendly manner. Table 2 displays the morphological overview which is used to generate the different concepts. The cross-sections are applied in the places as indicated by the yellow boxes in Figure 4.



Table 2 Morphological Overview

Function	Method 1	Method 2	Method 3	Method 4	Method 5	Method 6	Method 7
Connection in the wrist	Bayonet 	Thread 	Omega 	Pyramid Adapter 	Clamped 	Quick Lock Pin 	
Additional connection method	Bolt and nut 	Set screw 	None 				
Change position hand/adaptor	Bayonet 	Thread 	Omega 	Pyramid Adapter 	Spherical Joint 	Clamped 	Fixed Slots 
Connection below elbow (transhumeral)	Bayonet 	Thread 	Bolted 	Omega 	Clamped 	Set Screw 	
Connection above elbow (transhumeral)	Bayonet 	Thread 	Bolted 	Omega 	Clamped 	Set Screw 	
Concepts	I	II	III	IV	V	VI	

When the concepts are selected, CAD models are generated for each of the concepts to highlight the most important mechanics of that concept. By doing so, the concepts become subject to objective testing and scoring. This leads to the selection of the most promising design which optimally aligns with the predefined criteria.

### 2.2.3. Criteria

#### Finite Element Analysis

The subsequent stage in the design process entails testing and assessment of the developed concepts. By this point, CAD models of the concepts have been created, enabling the utilization of Finite Element Analysis (FEA) for each of them. FEA constitutes a powerful numerical simulation technique employed to comprehensively scrutinize stresses, strains, and deformations under varying conditions. This analytical approach provides invaluable insights into the performance of the connection methods. FEA serves as a virtual laboratory for assessing how the connection methods behave under different loads and stress conditions. It offers the following critical advantages:

- **Stress:** This parameter quantifies the internal force experienced by a material due to an external load. Stress is calculated for each element within the mesh model, and the results are instrumental in identifying the most heavily stressed regions within the structure. This value (MPa) must remain below the yield strength threshold as discussed above.
- **Displacement:** This measures the extent to which a material undergoes movement in response to an external load. In addition to assessing stress about design strength, structural

function failure can also result from factors such as deformations or deflection. These results aid in understanding how much the structure deforms under load.

- **Strain:** This parameter quantifies the degree of deformation experienced by a material due to an external load. The outcomes provide insights into the extent of material deformation under load.

It is worth noting that FEA is typically applied to solid parts, and several assumptions were made for the FEA of AM parts to ensure accurate and meaningful results:

- **Materials Behaviour**  
The analysis assumes that the material remains within the elastic region, with the yield stress set at 20 MPa for Tough PLA, as plastic deformations occur beyond this point. The maximum stress should remain below the material's strength. This is an essential consideration for assessing the prosthetic's mechanical performance and safety margins.
- **Static Stress Analysis**  
Von Mises analysis is utilized, particularly when increasing the load on the forearm. However, it is acknowledged that this method may not always provide precise results for plastics. To enhance accuracy, friction coefficients between the plastic components are meticulously evaluated.
- **Solid Body Assumption**  
The FEA model assumes that the connection methods are completely solid, providing a simplified yet practical representation for analysis.

The initial phase involved applying FEA to the forearms of the concepts, primarily due to the forearm's crucial role as a load-bearing component in the prosthetic device. This FEA process provided a thorough evaluation of mechanical performance, including stresses, displacements, and strains, along with the identification of potential weak points. This emphasis on the forearm is vital because it directly influences the functionality, structural integrity, and safety of the prosthetic device.

In these analyses of the forearm across all concepts, the forearm was firmly secured at its proximal end, while a 100 N force (approximately 10 kg) was applied to the distal end, enabling a detailed examination of the mechanical performance and structural aspects.

Utilizing FEA to assess these mechanical factors across every element within the model allowed for a comprehensive understanding of how the forearm would perform under various loads and conditions. This enabled the optimization of the forearm to maximize strength and rigidity, all while minimizing material usage and associated costs.

### Variable Requirements

Besides the results from the FEA, the concepts are also scored through the variable requirements and their weights accordingly. The top 3 weighted requirements are:

1. **Fu – As 3:** The connection methods allow for one-handed assembly.
2. **Fa - Re 2:** The prosthetic device is compatible with 3D printing technology.
3. **Fu – As 2:** The prosthetic device allows the patient to assemble the prosthetic device in less than 10 steps.

Per requirement, each concept can score 1 – (4\*requirement weight). Here, 1 means sufficient whereas 4 means excellent. Alternatives that satisfy poorly, scoring less than sufficient, are not alternatives and should therefore be discarded [14]. As the requirements are divided into two



sections, functional and fabrication, it is possible to differentiate between the concept scores per section. The establishment of the scores can be found in Table 3.

Table 3 Assessment for scoring

Code	Assessment
<i>Fu – As 2</i>	Score = (12+3)-#steps
<i>Fu – As 3</i>	Screw = -2 Bolt = -3 Connection Aid = +1
<i>Fa – Co 1</i>	Bolt = -1 Clamp/ Metal Tube = -2
<i>Fa – Re 2</i>	Non-Plastic = -1
<i>Fa – We 1</i>	Weight < 350 gram = 8 Every +25 gram range = -1
<i>Fa – We 2</i>	No support = 4 Weight ratio = 1 for hand-printed with and without support = 3 Weight ratio > 1 for hand-printed with and without support = 2

#### 2.2.4. Final concept selection

By placing the results of the requirements in a S(Stärke)-Diagram, German for “Strength”, it can be shown which concept is best according to functional and fabrication requirements (the concept which is closest to the diagonal line). Figure 5 shows the S-Diagram which will be filled in based on the ratings. Here, the redline indicates the minimum border which in this case is set by the x- and y-value of 40% and by (x+y)-value of 55%. The visual representation in this diagram allows for easy observation of the area in which improvements must take place, so the functional or fabrication side. Selecting a final concept to further work out does not mean that the rest of the concepts are neglected. It is possible to use some components of those concepts and integrate them with the final concept.

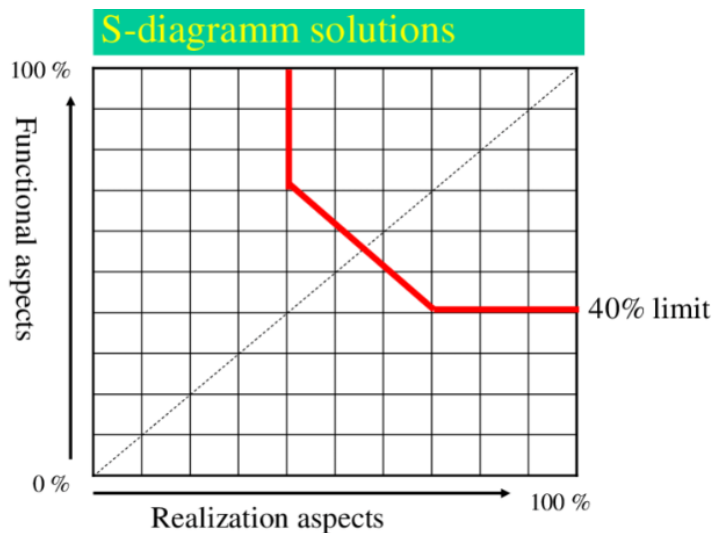


Figure 5 S-Diagram illustrates how the different concepts score on functional and fabrication(realization) levels

## 2.3. Testing Procedures

### 2.3.1. FEA Simulations

#### Static Load

When the final concept is selected, FEA analysis is extended to the wrist and the upper part of the elbow modules. If the analysis reveals stress levels approaching or exceeding the material's yield strength (20MPa), necessary modifications are introduced to alleviate these stress concentrations. This is done using the method that the stresses are calculated in the device. In the example of the forearm, the force (F [N]) which is applied on the forearm as well as the length (L [m]) of the forearm remain constant. Filling this in for the formula brings the bending moment (M [Nm]):

$$M = \frac{FL}{4}$$

This value is used in FEA to calculate the local stress which occurs due to the load F. The stress,  $\sigma$  [ $N/m^2$ ], is calculated as:

$$\sigma = \frac{Mc}{I}$$

Here, "c" [m] is the maximum distance from the centreline to the outer edge and "I" [ $m^4$ ] is the moment of inertia. "c" changes over the length of the forearm, but will remain the same within that range as the outer part of the forearm will not be adjusted. It is found that the value of "I" needs to be increased to reduce the stresses. "I" can be found for circular cross-section with outer and inner radius ( $r_o$  [m] and  $r_i$  [m]) as follows:

$$I = \frac{\pi(r_o^4 - r_i^4)}{4}$$

So when the stresses of the parts are operating around or above the yield strength, we need to increase the value of "I" by either changing the cross-sectional shape, increasing the material thickness or changing the geometry.

However, there is a limit to this increase, as by increasing this value the weight of the device also increases. So to ensure the patient has a light prosthetic device which is comfortable to use and functional, a balance must be found between the strength of the device and the weight. To further reduce the stresses, sharp edges and small areas will be avoided.

Furthermore, strength can also be influenced by adjusting parameters for FDM as found in subchapter 2.1.1 Production Process.

#### Fatigue Analysis

In addition to static analysis, fatigue analysis was conducted to estimate the product's service life. While static analysis is suitable for assessing single-use scenarios, the prosthetic device endures repetitive usage. This fatigue study was aimed at determining the product's durability over time. In fatigue analysis, the stress (represented by S) and the number of load cycles until failure (denoted as N) are critical factors. When the fatigue limit is established, it implies that the product's life duration (under load) is theoretically infinite for any stress below this limit. The specific load case R=-1 was considered. This case is fully reversed and here the load cycles start from a neutral position, proceeding downwards, then return to the neutral position after which the cycles move upwards before finally returning to the neutral position.

The established S-N curve of PLA is illustrated in Figure 6 [29].

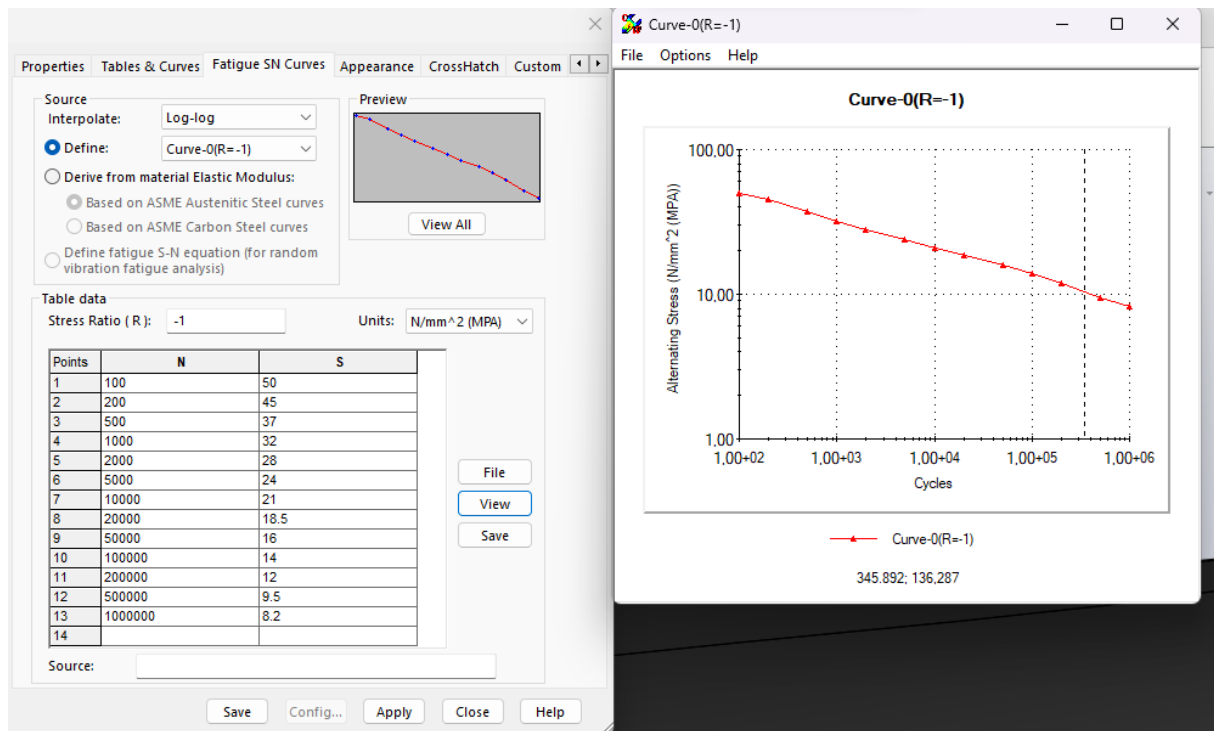


Figure 6 S-N curve added for PLA based on the mean stresses for 0°, 45°, and 90° orientation ( $\theta_{f}$ )

Subsequently, prototypes of the connections are 3D printed, and their performance is assessed during the proof-of-concept phase.

### 2.3.2. Physical Testing

Once the simulations are completed, and the connections meet their intended criteria, physical testing ensues. The strength of the upper limb prosthetic is systematically examined following ISO-22523:2006(E) standards, titled “External Limb Prostheses and External Orthoses Requirements and Test Methods”. This concludes testing for the following categories:

- **Proof strength:** the static load representing an occasional severe event, which can be sustained and still allow the prosthetic or orthotic device to function as intended.
  - This load is given as a requirement and is 98.1N (for simplicity 100N).
- **Ultimate strength:** the static load representing a gross single event, which can be sustained but might render the prosthetic or orthotic device unusable thereafter.
  - This load is the load of the proof strength with a safety factor of 2 applied, resulting in 196.2N (for simplicity 200N).

The method of testing the strength of upper-limb prosthetic devices is based on a series of laboratory tests consisting of a static tensile test, and static and cyclic downward and upward bending tests. As the focus lies on the strength of the connection methods in the wrist and the proximal part of the forearm, the test focuses on the forearm. Here, the upper part of the elbow is assumed, which contain the same connection method as below the elbow, to withstand the same forces and therefore will behave the same as the connection below the elbow module. Another reason to not include the elbow module in the test is that the elbow module can withstand a maximum of 98.1N [9]. This indicates that the locking elbow will succumb sooner compared to the connection in the upper elbow part, this would mean that it is not able to find the ultimate strength of the connections.

The test performed for the upper arm is the distal strength test. Here, the test is performed by adding a load, to the hand while the forearm is attached to a mounting block on a flat vertical surface as depicted in Figure 7. The applied load starts with a load of 1kg and increases with 0.5 kg up to the required load of 10 kg. Then the load is removed and the part will be checked for cracks or deformations using a visual inspection. After this, the required load is applied once more and the load keeps on increasing up to the load which is considered for the proof strength of 196.2N.

If the device does not break at this point, the device is once more checked visually for cracks and deformations. In this case, the load continues to increase until the part finally breaks, resulting in the ultimate strength.

This test method is applied for both the new concept and the current glued design. By this means, the strength of the new concept can be compared with the results of the glued device, which indicates if the strength of the new arm is increased or decreased besides the increase in modularity.



Figure 7 Test set-up.

Figure 8 illustrates a simplified situation of the test set-up. The table below gives the correct values for the positions and distances. Here, X is the distance the load is applied in the hand. We have here the mounting block (1), the forearm (2), and the hand (3).

Table 4 Positions and distances test set-up

Position	Length [mm]
I	20
II	166,55
III	140,26
X	305,15

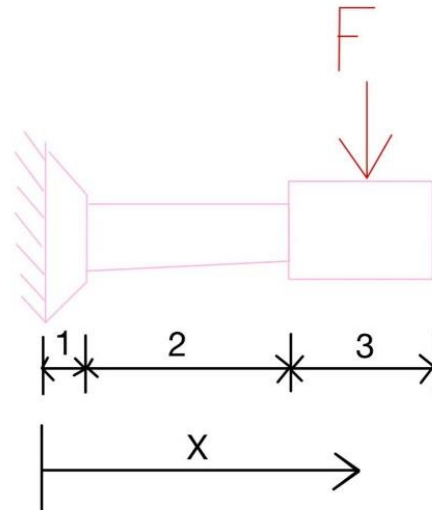




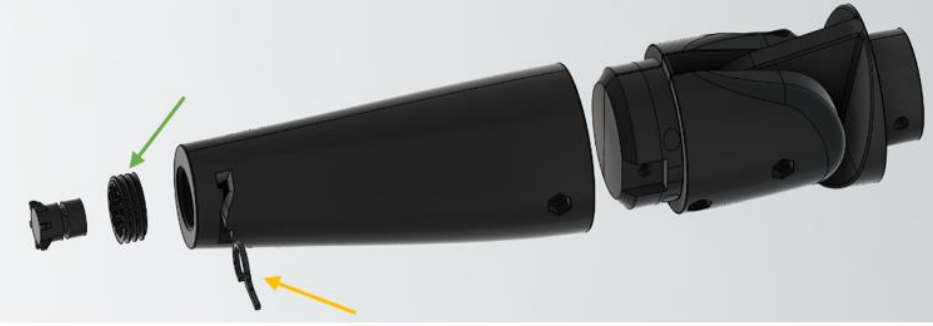
Figure 8 Simplified situation of the test set-up

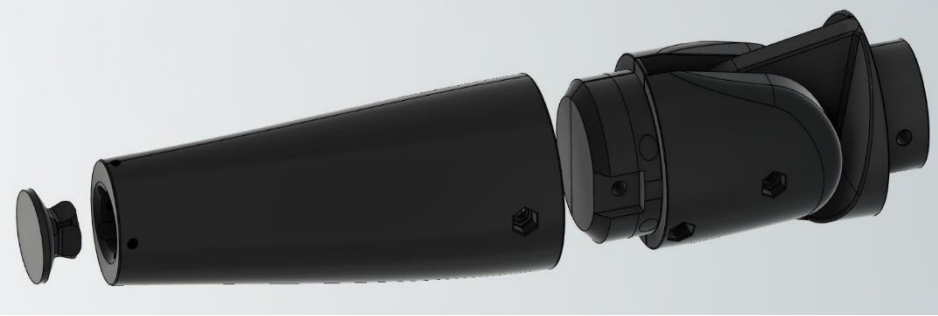
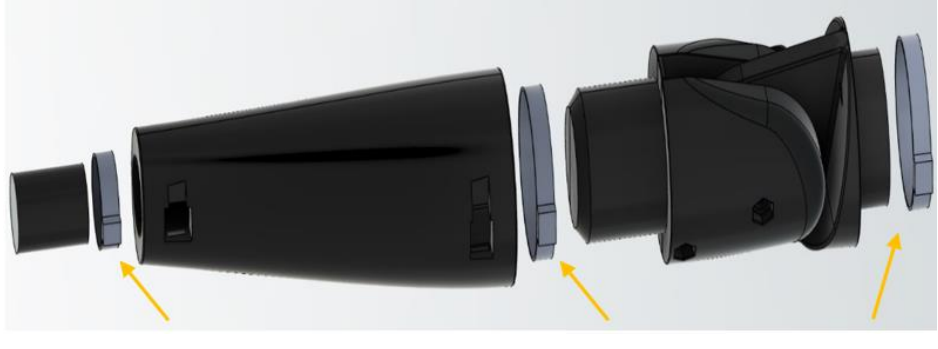

### 3. Results

#### 3.1. Concept Illustration

Utilizing the Morphological Overview in Table 2, a total of 6 concepts were generated. The different method combinations which resulted in the concepts are included in Appendix B: Morphological Overview Selected. Table 5 displays the CAD models of the different concepts employing an exploded view.

Table 5 Exploded view of the generated concepts

Concept	Exploded view of the concepts
<p><b>1 – Bayonet</b></p> <p>The focus lies on methods commonly used in prosthetics. The bayonet connection is used in the current printed design (upper part of the elbow to socket) but is now applied to all the connections. A bolt and a nut are included to lock the bayonet connections in place.</p>	
<p><b>2 – Threaded</b></p> <p>This concept focuses on rigidity. The connections are realized using threads and the position of the adapter in the hand can be locked using the set screw, indicated by the yellow arrow, which is pressed against the adapter. The slot in the adapter allows for 180° rotation in the wrist.</p>	
<p><b>3 – Omega</b></p> <p>The focus of this concept is the ease of operating the wrist. The elbow module is locked using bolts and nuts while the wrist module is locked using a torsion spring, indicated by the yellow arrow. This allows for easy (un)locking of the adapter of the hand. The thread, referred to as guidance and indicated by the green arrow, locks the adapter in the axial rotation.</p>	

<p><b>4 – Pyramid</b></p> <p>The focus lies on methods commonly used in prosthetics. The pyramid adapter in the wrist is commonly implemented in leg prosthetics. The elbow module is locked using bolts and nuts.</p>	
<p><b>5 – Clamped</b></p> <p>The focus of this concept is rigidity. The parts are connected and clamped using hose clamps, indicated by the yellow arrows. This allows for 360° rotation in the wrist adapter.</p>	
<p><b>6 – Quick Lock Pin</b></p> <p>This concept focuses on the ease of operating the wrist. The elbow module is locked using bolts and nuts while the adapter of the wrist can be locked using a quick lock pin. The pin operates in the predetermined slots in the adapter of the wrist. This allows easy (un)locking of the adapter.</p>	

### 3.1.1. Initial Strength Exploration Forearm of the Concepts

The figure below illustrates the FEA analysis result regarding stress for the threaded concept, concept 2. It is worth noting that the stresses in the proximal part of the forearm do not exceed the threshold of  $2.000e+01$  MPa and thereby, theoretically, meet the requirement to withstand a load of 100N.

The FEA results of the other concepts (stress, displacement, and strain) can be found in Appendix C: FEA for the Concepts.

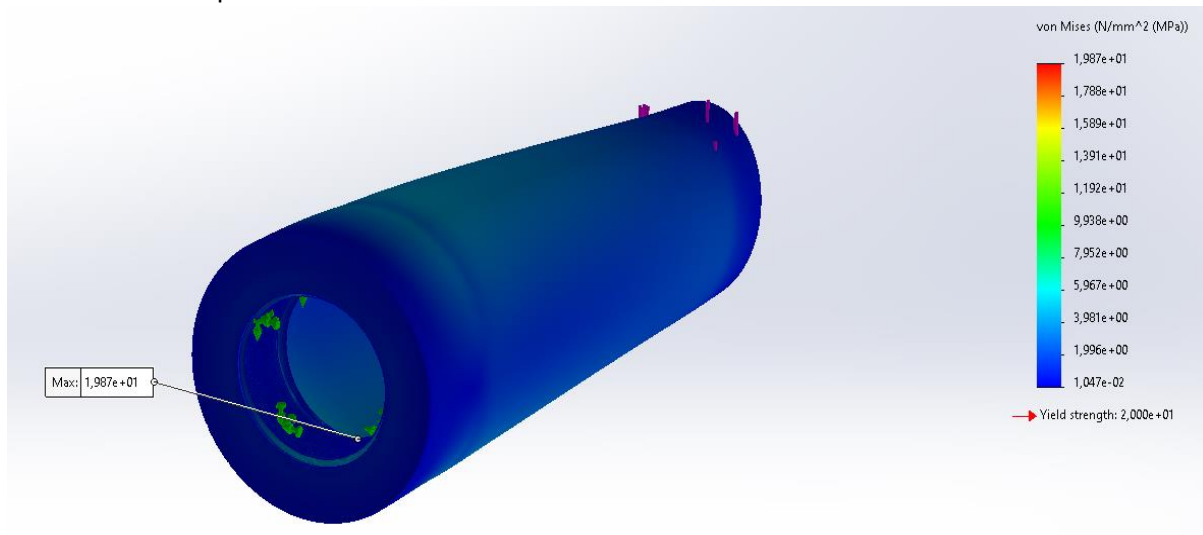


Figure 9 Stresses in the threaded concept by applying 100N on the distal end and locking at the proximal side. Maximum stress here is  $1.987e+01$  MPa which occurs in the proximal thread.

### 3.1.2. Concept Selection

The scores per variable requirement can be found in Appendix D: Scoring Tables.

These scores are visualised using the S-diagram as shown in Figure 10. This diagram displays how much percentage per section each concept contains. The dotted line displays the 50% - threshold line. Concepts that fall outside this section are left out for the final concept choice. Since concepts 2 (threaded) and 3 (omega) fall in this threshold, their key parts will be considered for the final concept. By improving some parts of the concepts and by combining parts that work best, the final concept score will be placed towards the top-right corner.

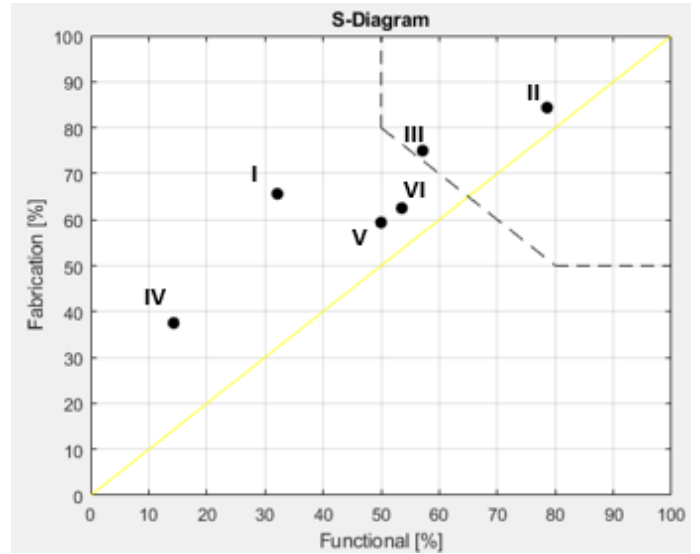
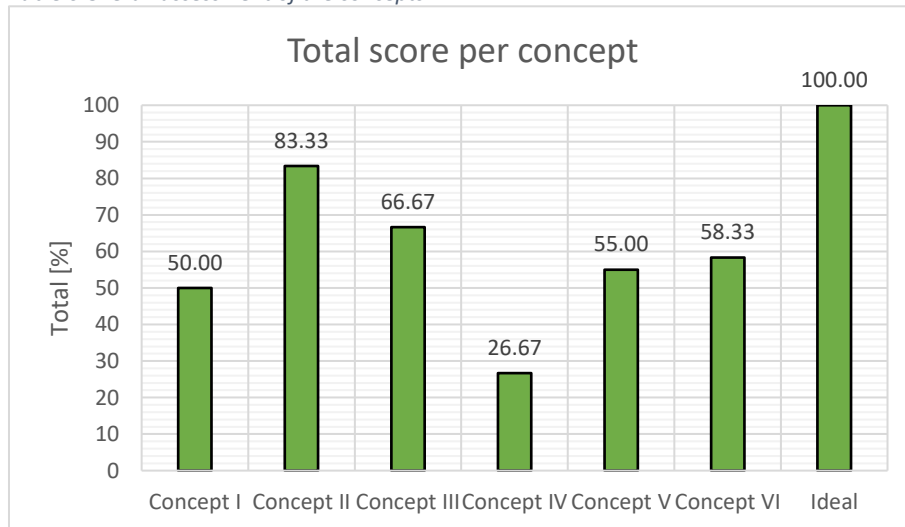


Figure 10 S-Diagram for the Kesselring Method. The yellow line indicates a perfect score based on the fabrication and functional requirements. The dotted section in the top right corner indicates the 50% threshold.

The S-diagram shows how well the concepts score on the sections. However, it is hard to see how the concepts score overall. For this, the overall score is determined. The concept score in total on the variable requirements can be seen in Table 6. Here, it is shown, just as in Figure 10, that the threaded concept (concept 2) scores highest in general and the omega concept (concept 3) comes in second.

Table 6 Overall assessment of the concepts



### 3.1.3. Concept Selection

Based on the rigorous evaluation and scoring performed using the Kesselring method in conjunction with the detailed FEA results, the threaded concept (concept 2) emerged as the best-performing candidate. As stated earlier, the focus of this concept lies in its rigidity. To promote the ease of changing and repositioning the adapter for the patient, the wrist component of the omega concept (concept 3) is also investigated as the focus of this concept is the ease of operating the wrist. Furthermore, this concept is selected as it also scores second highest on the variable requirements. The synergy between the quantitative evaluation and the simulation data identified these concepts as the most promising choices for further development and prototyping. This selection is based on their exceptional performance on critical criteria that closely align with project goals and the



demanding requirements of a resource-constrained environment. As a result, the threaded concept and the wrist module of the omega concept now take priority and will be the focus of subsequent research phases.

Moreover, it's worth noting that although a few alternative concepts exhibited better performance in the FEA than the omega concept, their overall scoring using the Kesselring method did not meet the required standards. As a consequence, these particular concepts were excluded from further consideration and prototyping.

### 3.2. Iterative Development

As the threaded concept scored best overall, this concept is selected as the basic concept. The focus of this concept is the rigidity. To see what the strengths and weaknesses are, this concept is first completely finalized and tested. This is done using Proof of Concepts in which the connection parts of the concept are printed to see how the mechanism works. By doing this, mechanics that do not work can be found easily and problems which are not thought of before also come to light.

This subchapter focuses on the iteration steps of the final concept. To come to this solution, the threaded concept and omega concept are first thoroughly examined and tested. The iteration steps of these two concepts can be found in Appendix E: Iterative Steps. In these steps, the concepts are tested using Proof of Concepts. The results for both concepts can be found in Appendix F: Proof of Concepts

#### 3.2.1. Threaded connections

As stated before incorporates the basic concept of a threaded mechanism within the wrist, and on both sides of the elbow module, see Figure 11. The upper and lower elbow modules can be precisely adjusted to accommodate the forearm and secure the socket to the elbow. Within the hand component, an adapter featuring external threading is designed for insertion into the wrist assembly, as indicated in the figure by the black arrow. This adapter can be securely positioned by utilizing a set screw, indicated by the yellow arrow. To safeguard the integrity of the threading, three strategically placed gaps, distributed over 180° along the thread pitch, are incorporated. This precautionary measure effectively prevents thread damage caused by the set screw. Figure 12 shows the connections between the wrist and elbow utilizing a sectional analysis.



Figure 11 Threaded concept; From left to right are the wrist adapter (black arrow), the forearm with the set screw (yellow arrow), and the elbow module on the right.

The hand (placed on the adapter of the wrist) is left out for overview purposes.



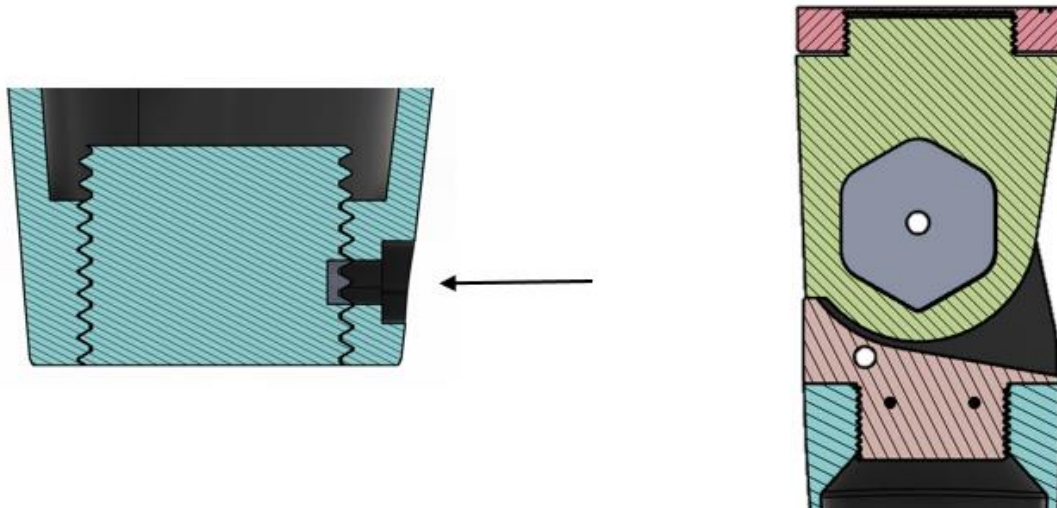


Figure 12 Front view wrist module and side view distal/ proximal ends of the elbow module. The black arrow shows the insertion of the set screw for the wrist module (yellow arrow in Figure 11). The holes in the elbow module are for the assembly of the elbow using bolts and nuts. The top part of the elbow module allows for connection to the socket of the transhumeral amputated arm.

### Thread optimisation

Initially, a pitch of 2 mm and a diameter of 45 mm was employed in the proximal thread. This proved to be working near the yield stress region,  $2.000e+01$ MPa, when a load of 100 N was applied, namely  $1.987e+01$  MPa. To overcome this, the pitch was revised to 5 mm and the diameter to 48 mm, ensuring greater durability and load-bearing capacity. This adjustment allowed the thread to withstand higher loads in the perpendicular axis, as the stresses in the proximal threaded part dropped significantly for the applied load of 100N, see Figure 13.

The distal thread needed more refinement as the thread size was smaller. Eventually, an offset of -0.2mm and a fillet of 0.25mm are applied on the thread to overcome the tolerances for the thread using this production method. The displacements and strain in the proximal part as well as the wrist of the adjusted threaded concept can be found in Appendix G.1. Additional FEA - Threaded Concept. This concept is ready to be physically tested to examine the real-world responses to the applied load.

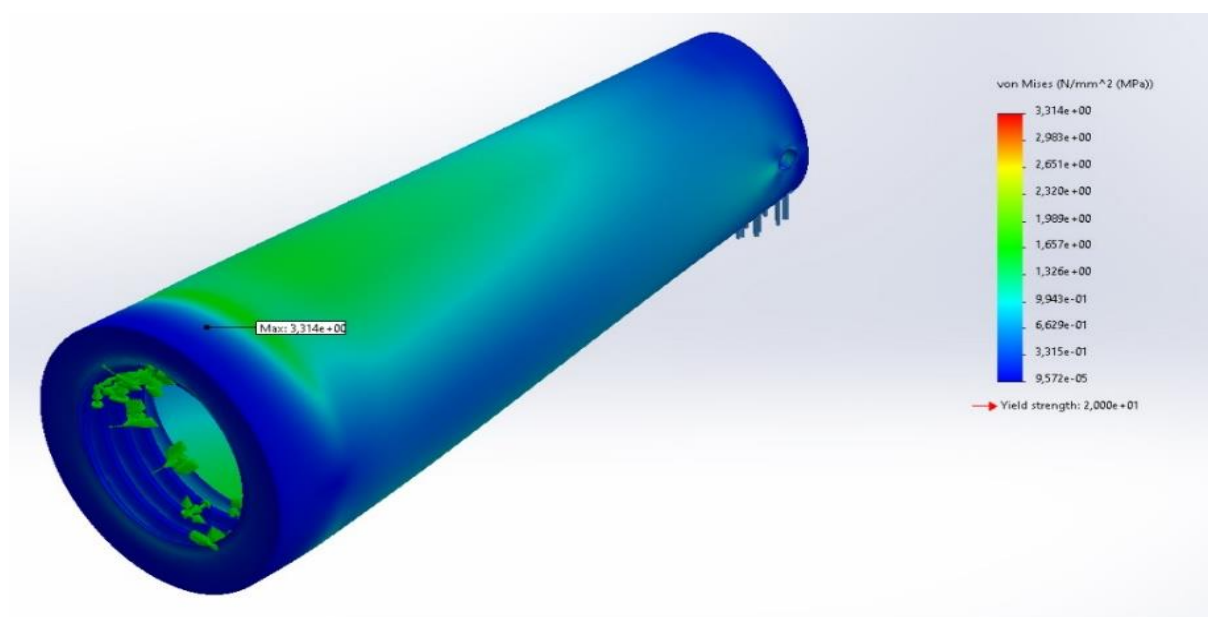


Figure 13 FEA for adjusted proximal part of the threaded concept. Here the maximal stresses which occur when a load of 100N is applied perpendicular at the distal end is  $3.314e+00$  MPa.

### Physical testing

The test is conducted in an environment with 22.6 °C and a humidity of 72%. Here, a load is applied by placing weights of 1 kg up to the required 10 kg. This load was applied for 2 hours, after which no physical deformations were observed. The load was increased up to 30.5 kg, which was applied for 2 hours. Once more, no physical deformations were observed. Next, the weight kept increasing up to 62.9 kg. At this load, the wrist broke in the adapter as seen in Figure 14. Given the value at which the adapter broke, the maximum torque in the wrist is found as:

$$62.9\text{kg} \cdot 9.81\text{m/s}^2 \cdot 0.1186\text{m} = 73.18\text{Nm}.$$

No physical deformations were found in the thread on the distal and proximal parts of the forearm.

### Concept evaluation

The current method employed for the connections on both sides of the forearm demonstrates effectiveness and high strength in many aspects. However, a significant bottleneck emerges in the wrist due to the necessity of using a metal set screw within this configuration. The interaction of metal screws with plastic components can lead to various issues, including the risk of structural damage in the thread applied by the metal set screw. Such wear and tear over time can have adverse effects on the integrity of the connection, necessitating maintenance or replacements, which in turn result in additional costs. To overcome this, the wrist connection of the omega concept (concept 3) is investigated.

#### 3.2.2. Wrist Adaptation

The wrist module of the omega concept (concept 3) is based on the omega wrist module of Fillauer TRS Inc [30], see Figure 15. This method is adjusted for FDM technology in which some of the parts can be combined to reduce the total amount of parts.

The wrist module makes use of a torsion spring, an adapter and guidance, these parts are indicated by the arrows and labelled 1, 2 and 3 respectively in Figure 16. The torsion spring is placed into the cavity after which the guidance is screwed into the forearm. The torsion spring is opened after which the adapter can be placed in the guidance ring. As the adapter contains notches, the rotation is limited due to the grooves in the guidance ring. When the torsion spring is closed, the inner diameter reduces which makes it clamp around the groove placed in the shaft. The forearm and socket are connected to the elbow module using bolts and nuts.



Figure 14 Testing of threaded concept. The location of breakage in the wrist adapter after an applied load of 62.9 kg.



Figure 15 Omega Wrist Fillauer TRS Inc.

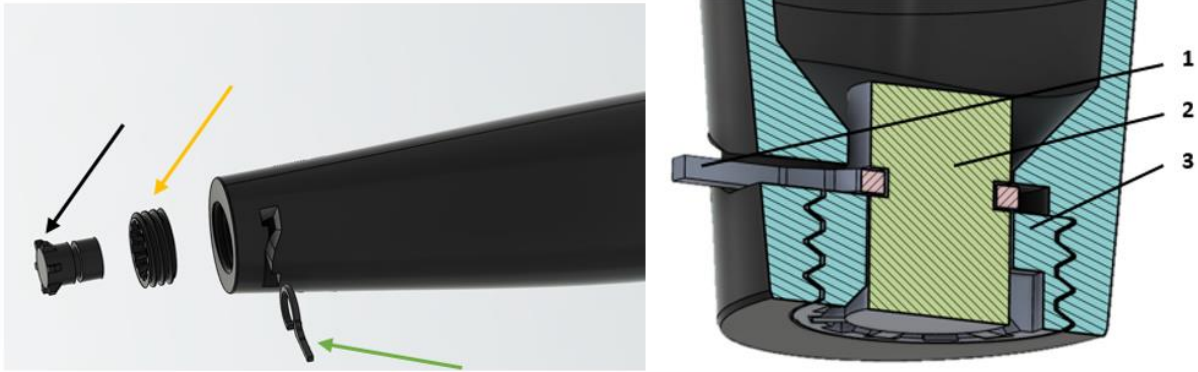


Figure 16 Wrist adaptation from concept 3 – Omega;

Left figure: From left to right are the wrist adapter (black arrow), the guidance (yellow arrow), and the forearm with the torsion spring (green arrow).

Right figure: Side view wrist module. The numbers in the wrist module are: 1. Torsion Spring; 2. Adapter; 3. Guidance.

### Physical testing

This concept is tested at 23.6°C and a humidity of 73%. Here, a load is applied by placing a load of 1 kg up to the required 10 kg. When this succeeded, the load was applied for 2 hours. After this, no physical deformations were observed. The load was increased to 17.5 kg. This load was applied for 2 hours.

During these 2 hours, no gap was observed in the proximal end of the forearm. However, gaps occurred in the wrist, see Figure 17. After this observation, the load was removed and the torsion spring was evaluated. The torsion spring contained white regions where the stresses applied by opening and closing the torsion spring were too high for the material to deform plastically. This already occurred before applying the load of 17.5 kg. Furthermore, the torsion spring was bent due to the high load. The testing was stopped as the torsion spring would not be able to withstand more loads or the same load of 17.5 kg.



Figure 17 Testing of the combined concepts with a load of 17.5 kg for 2 hours.

Left illustrates the gap in the wrist module during the test;

Right shows the torsion spring after the test. Here the white parts are results of the stresses which occurred during the opening and closing of the pin.

### Concept Evaluation

A notable strength of this concept lies in the ease of inserting, adapting the position, and removing the hand and its adapter. By applying the settings for the threads found in the threaded concept, a reliable and secure connection mechanism is applied in the wrist module.

It is important to address the weakness of this design. As the thread of the threaded concept is wider than the adapter in this concept, it can be concluded that this connection method will be able to succumb under a lower load than concept 2. Increasing the adapter in this concept will reduce the

body between the thread and the wall of the forearm. This is unwanted as it will be able to cope with less loads.

The torsion spring is another weakness in the design, despite it being initially chosen for its functionality. It struggles to handle the stresses associated with opening and closing, which is a crucial aspect of its operation. Furthermore, it fails to perfectly lock the adapter in the z-axis as the gaps in the wrist occur. This calls for a more robust spring or alternative locking mechanism to be implemented.

### 3.3. Glued Connections

The prosthetic arm with the connection method that is currently used in Sierra Leone is also physically tested. The connections are glued with instant glue. The arm was tested at a temperature of 22.6°C and a humidity of 72%. Eventually, the load at which the threaded concept broke was attached and the arm did not break. Still, no deformations were seen after the load of 65 kg was removed. The testing was stopped as the threaded concept already broke at this weight.

The torque in the wrist at which the testing was stopped is found at:

$$65\text{kg} \cdot 9.81\text{m/s}^2 \cdot 0.1186\text{m} = 75.63\text{Nm}.$$

### 3.4. Final Concept

The final solution to overcome the problems was the use of a tube clip. This would be clipped around the shaft to lock the z-axis. As the rotation is already locked through the guidance, the hand would indeed be locked in place. It was found that it was best if the tube clip circle was enclosed, reducing the chance of falling out and losing the clip when the clip was removed. However, this addition to the clip made it impossible to stay on the inner side of the forearm where the torsion spring was located. Therefore, the tube clip is placed on the side. The upper side is chosen because it would be easy to bump into it when the clip is on the lower side, as well as the way the load is applied onto the hand. When the tube clip is placed on the upper side, the shaft is better clamped as most of the forces are applied in the z-axis. Figure 18 illustrates the exploded view of the combined concept including the tube clip.

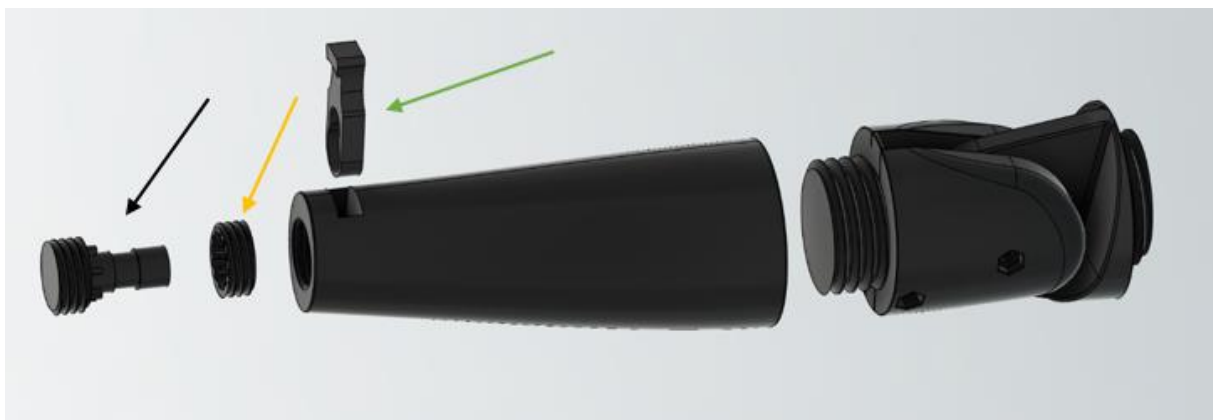


Figure 18 Final concept – Combination of the threaded and omega concepts; From left to right are the wrist adapter (black arrow), the guidance (yellow arrow), the forearm with the tube clip (green arrow), and the elbow module on the right.



## Adapter optimisation

It is observed in the previous tests that the adapter fails before the hand does. To reduce print time and costs, the adapter is made as a separate part which can be inserted into the hand. This allows that the adapter only needs to be printed when the adapter breaks instead of the adapter and the hand. The diameter of the shaft which is locked by the tube clip is also increased from 10 mm to 12.50 mm which increases the strength of the part by a factor of 30% when a load of 200N is applied, see Figure 19. By this means, the adapter would fulfil the safety factor of 2.

The increase of 2.5mm in the shaft of the adapter was the maximum the shaft could increase. Otherwise, the adapter would lose the function to lock the rotation in the z-axis due to too low interacting parts. Furthermore, the area of the shaft which interlocks with the tube clip could not increase more as there would then be no gap between the interlocking part and the outer part of the shaft for the tube clip to grip on.

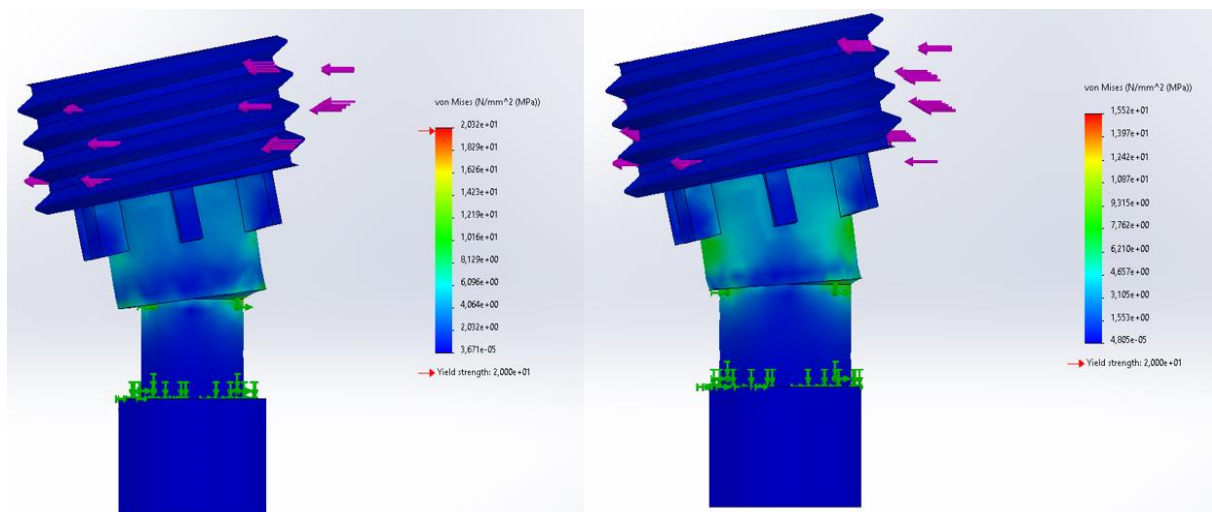


Figure 19 FEA of the adapter for different shaft diameters with a load of 200 N fulfilling the safety factor of 2:  
Left 10 mm with a maximum stress of  $2.032e+01$ MPa;  
Right 12.50 mm with a maximum stress of  $1.552e+01$ MPa.

The thread on the adapter is implemented with the same settings as the threaded connection in the wrist of the threaded concept. As this thread is self-locking, no set screw needs to be applied. An additional tool is designed and 3D printed which allows for easy removal of the adapter when the shaft breaks, as well as the removal of the guidance, see Figure 20.



Figure 20 3D printed tool to tighten and remove the adapter in the hand (hole on the left); the guidance in the forearm (height on the right)

## Physical testing

This concept is tested with 22.1°C and humidity of 71%. Again, loads are applied by a load of 1 kg up to the required 10kg. This load was once more applied for 2 hours. Hereafter, no physical deformations were observed. The load was increased to 17.5 kg as the test for the torsion spring stopped at this load. This load was applied for two hours. After the two hours, no deformations were observed. Eventually, the adapter broke at 22.5 kg. The printed tool was used to remove the adapter. The threads were analysed which did not show deformations.

A new adapter was inserted and the test was performed once more in the same order to see if the results decreased. The new adapter once more broke at 22.5 kg after which no deformations in the arm and other parts were found.

For this concept, the torque at which the adapter broke is found as:  $21.7\text{kg} \cdot 9.81\text{m/s}^2 \cdot 0.1186\text{m} = 26.18\text{Nm}$ .

### Concept evaluation

Although this concept is significantly less strong compared to the threaded concept, the modularity is increased and this concept is more patient-friendly due to the ease of operating the tube clip and repositioning the hand with one hand. Furthermore, this concept eliminates the need for metallic parts which are pressed on plastic components. Finally, the thread on top of the adapter allows for ease of replacement when the adapter breaks.



Figure 21 Broken adapter of the newly selected concept. No deformations are found in the hand and thread

### 3.5. Concept Score

The physical testing results of the final concept indicate that the load at which the concept broke is lower than the load at which the threaded concept broke. However, the ease of operating the adapter for the patient is improved and the hand does not need to be reprinted when the adapter fails. The final concept is subjected to the variable requirements to see if the combination of the threaded and omega concepts with corresponding adjustments indeed scores best.

By combining the best parts of both concepts, assembly steps were reduced and the parts which could not be 3D printed now became zero. The new S-Diagram with this final concept (concept VII) included as well as the new scoring table can be seen in Figure 22 and Table 7. The new scoring tables can be found in Appendix H: Final Scoring Tables.

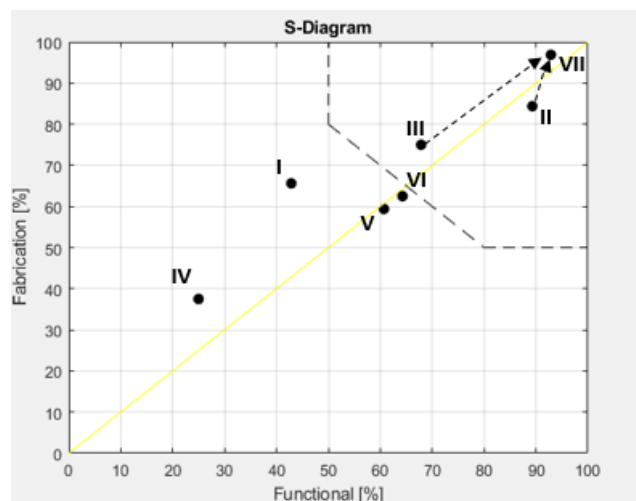
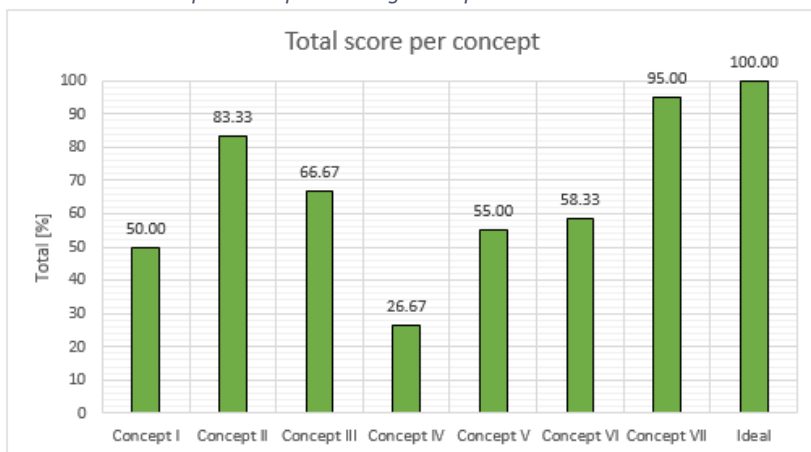


Figure 22 S-Diagram including concept VII which is a combination of concepts II and III

Table 7 Total score per concept including Concept VII



## 4. Discussion

### Main findings

The key findings of this research revolve around the development of connection methods for 3D-printed upper limb prostheses, emphasizing functionality, adaptability, and safety in low- and middle-income countries. The chosen concept prioritizes modularity and user-friendliness, catering to the need for adaptable and accessible prosthetic solutions in such settings. Rigorous FEA and physical testing validate the concept's viability.

The final concept exhibits remarkable adaptability and improved modularity, crucial for the case study. While the threaded concept excels in mechanical strength and durability, it poses a trade-off between modularity and strength. The final concept prioritizes patient usability, removes metal-on-plastic components, and ensures safety with a 2x safety factor. Balancing modularity, strength, and longevity, the final concept emerges as a more suitable choice for low- and middle-income countries, addressing the unique needs of patients in those settings.

### Iterative design steps

During the iterative design process, the findings made the importance of paying attention to tolerances clear. Each iteration of the design led to valuable insights and highlighted the need for accurate tolerances to ensure optimal functionality and compatibility. Adjustments to the screw configuration were important to address challenges during testing, illustrating the iterative nature of the design process. In particular, changes in screw sizes and configurations were critical to optimizing the connections. The evolution of the design, which carefully considered tolerances and screw characteristics, attests to the iterative nature of refining connection solutions, which ultimately contributed to the development of a more robust and effective final concept.

#### *The set screw in threaded concept*

In the earlier iterations of the threaded concept, efforts were made to improve its functionality by introducing a set screw to secure the hand. Although this modification allowed for a 180° revolution to lock the hand, concerns arose about the potential impact of metallic pressure on the plastic, resulting in a reduced lifespan for the adapter.

During the exploration of 3D printing as an alternative solution, distinctive challenges came to light. A crucial aspect was ensuring the preservation of thread integrity within 3D-printed components. The inherent limitations in the resolution of printing technology became apparent, posing potential obstacles to accurately replicating the required threads. The use of fine threads, essential for this connection, increased the risk of breakage during use. Furthermore, the incorporation of a metal screw into the 3D-printed structure would likely require an additional step of tapping the hole, introducing complexity and escalating manufacturing costs.

### User testing

The absence of patient testing in this study represents a notable limitation, highlighting the imperative need for future research to involve amputees in the evaluation of the prosthetic device. To address this, it is suggested to implement a comprehensive user testing protocol that includes extensive interaction with amputee participants in real-world scenarios. Conducting user testing in collaboration with healthcare professionals and prosthetic users at the Masanga Hospital can offer valuable insights into the device's practical performance, comfort, and usability.

Furthermore, a structured follow-up questionnaire distributed to participants after a defined period of prosthesis use can gather detailed feedback on their experience. Questions should encompass aspects like comfort, adaptability, and challenges faced during daily activities. This user-driven

feedback loop can provide actionable insights for refining the prosthetic design and addressing specific user needs.

Engaging amputees in the testing process ensures the device's functionality in real-world conditions. This approach is essential for tailoring the prosthetic solution to the unique requirements of individual users, ultimately enhancing their quality of life. Integrating patient testing and feedback into future research will be critical in optimizing and refining the prosthetic design for maximum effectiveness and user satisfaction.

### **Differences between FEA and physical testing**

The FEA results for the threaded concept provided valuable insights into its design. Notably, the proximal forearm demonstrated robust strength, enduring a substantial load of 600N before approaching the yield strength. This resilience in the forearm design ensures the structural integrity required to support the entire prosthesis. Conversely, the wrist module exhibited a lower load threshold in the FEA analysis, around 100N, yet surprisingly endured forces up to 62 kg during physical testing—six times the anticipated threshold. Although there was a significant discrepancy in the load-bearing capacity, the FEA correctly identified the location of maximum stresses leading to failure, suggesting the wrist module's inherent robustness exceeded initial estimates.

The differences between FEA results and physical tests stem from various factors. A critical factor is the transition zone from the thread to the hand, characterized by a small cross-sectional area. Stress calculations consider the applied force divided by the area, resulting in higher calculated stresses in this region due to its small area. The simplification of the thread to a cylinder in a static load analysis, presented in Appendix I: FEA Simplified Wrist Adapter, showed increased load resistance from 100N to 300N. Additionally, during physical testing, the elastic yield strength of the material was exceeded, indicating that the prosthesis was operating in the plastic deformation region. This observation was not fully accounted for in FEA, where materials are often assumed to remain within their elastic limits.

Material properties play a crucial role, and the tensile strength at fracture of the prosthesis material, as reported by Merel et al. [8], was 37 MPa. This material property likely contributed to the disparities between simulation and physical test results, especially given the design was pushing the limits of yield strength. It's important to note that such variations between simulation and physical testing are not unique to this study, as evidenced by Abbott et al. [31], who found differences between the FEA of 3D printed models and compression testing results. They found that simulations with 50% infill represented almost double the displacement compared to dimensions with 100% infill, but the 3D-printed test specimens produced significantly different results. These considerations underscore the need for meticulous examination of material properties and potential plastic deformation in future FEA studies, especially when dealing with 3D printed materials.

### **Contribution of this research**

The results obtained from this study offer significant contributions to the advancement of upper limb prosthetics in resource-constrained third-world countries. While the primary focus was on designing and testing connection methods, the implications and practical applications of the findings extend to various aspects of prosthetic development and accessibility. These insights are invaluable for both researchers and practitioners in the field.

- **Enhanced Modularity**

The final concept, driven by its modularity, can be tailored to meet the unique needs of individual patients. This feature aligns well with the demands of our target application where patients may have varying requirements and where customization is crucial. Practitioners can



utilize this insight to design prosthetic systems that prioritize adaptability and user-friendliness, thus improving patient outcomes and satisfaction.

- **Mechanical Strength**

The remarkable strength exhibited by the screw fixation, especially in the proximal part of the forearm, is a noteworthy finding. This information can guide future studies in selecting materials and configurations that maximize durability and reliability, particularly for components that bear substantial loads.

- **Balance Between Modularity and Strength**

The trade-off identified between modularity and strength highlights the need for designers to carefully consider this balance when designing prosthetic devices. Researchers and designers can explore innovative ways to enhance both aspects without compromising one for the other.

## 5. Conclusion

To summarize, this research was initiated to develop and optimize upper limb prosthetic devices, tailor-made for the distinctive challenges in third-world countries. The fusion of advanced 3D printing technologies, modular design principles, finite element analysis, and rigorous physical testing has yielded invaluable insights and solutions. It is undeniable that 3D-printed prosthetics possess the potential to usher in substantial enhancements in the lives of limb loss patients in resource-limited regions, offering cost-effectiveness, adaptability, and a patient-centric, bespoke approach that brims with optimism.

Across both the S-Diagram and the comprehensive total score overview, a compelling narrative unfolds - the combined concept reigns supreme in addressing variable requirements, even though it exhibits slightly lower strength compared to the threaded concept. This evident edge in adaptability and patient-centred attributes solidifies its status as the most pragmatic choice.

Moreover, the findings emphasize the importance of a holistic approach. While finite element analysis illuminated the path to strength and resilience, rigorous physical testing provided essential real-world validation. The disparities between these two methodologies underscore the significance of continual physical testing and iterative design refinements. Furthermore, the importance of ensuring that the yield strength of a prosthetic design consistently remains well within the limits of the chosen material and design cannot be overstated.

### **Future Work**

While emerging as the most promising solution, the identified concept has yet to undergo the critical phase of patient testing. Consequently, it is strongly recommended that future research endeavours prioritize comprehensive patient trials complemented by corresponding questionnaires. The inclusion of patient-centric evaluations would undoubtedly enhance our understanding of the adaptability and usability of these prosthetic solutions in real-world scenarios. This crucial step will not only contribute to refining the design based on direct user feedback but will also ensure that the proposed prosthetic solution aligns seamlessly with the unique needs and preferences of individuals in diverse patient populations.

## References

- [1] H. E. M. A. Abbady *et al.*, “3D-printed prostheses in developing countries: A systematic review,” *Prosthet Orthot Int*, vol. 46, no. 1, pp. 19–30, Feb. 2022, doi: 10.1097/PXR.000000000000057.
- [2] J. M. Zuniga, A. M. Carson, J. M. Peck, T. Kalina, R. M. Srivastava, and K. Peck, “The development of a low-cost three-dimensional printed shoulder, arm, and hand prostheses for children,” *Prosthet Orthot Int*, vol. 41, no. 2, pp. 205–209, Apr. 2017, doi: 10.1177/0309364616640947.
- [3] C. S. Harkins, A. McGarry, and A. Buis, “Provision of prosthetic and orthotic services in low-income countries,” *Prosthet Orthot Int*, vol. 37, no. 5, pp. 353–361, Oct. 2013, doi: 10.1177/0309364612470963.
- [4] B. Cohen, “Urbanization in developing countries: Current trends, future projections, and key challenges for sustainability,” *Technol Soc*, vol. 28, no. 1–2, pp. 63–80, Jan. 2006, doi: 10.1016/j.techsoc.2005.10.005.
- [5] J. ten Kate, G. Smit, and P. Breedveld, “3D-printed upper limb prostheses: a review,” *Disability and Rehabilitation: Assistive Technology*, vol. 12, no. 3. Taylor and Francis Ltd, pp. 300–314, Apr. 03, 2017. doi: 10.1080/17483107.2016.1253117.
- [6] B. Maat, G. Smit, D. Plettenburg, and P. Breedveld, “Passive prosthetic hands and tools: A literature review,” *Prosthet Orthot Int*, vol. 42, no. 1, pp. 66–74, Feb. 2018, doi: 10.1177/0309364617691622.
- [7] J. J. , T. M. J. , P. P. A. , G. J. R. , S. M. , L. T. S. , . . . & S. B. T. Turcotte, “Limb amputations in Sierra Leone: A retrospective, observational study of 595 cases,” *PLoS One*, vol. 13, no. 11, 2018.
- [8] M. van der Stelt, L. Verhamme, C. H. Slump, L. Brouwers, and T. J. J. Maal, “Strength testing of low-cost 3D-printed transtibial prosthetic socket,” *Proc Inst Mech Eng H*, vol. 236, no. 3, pp. 367–375, Mar. 2022, doi: 10.1177/09544119211060092.
- [9] M. Kok, “Het Ontwerpen van een Transnumeraal Armprothese.”
- [10] P. de Graaf, “Thesis\_PiendeGraaf\_Transnumeraal”.
- [11] M. D. van Gaalen, M. van der Stelt, J. H. Vas Nunes, and L. Brouwers, “People with amputations in rural Sierra Leone: the impact of 3D-printed prostheses,” *BMJ Case Rep*, vol. 14, no. 6, p. e236213, Jun. 2021, doi: 10.1136/bcr-2020-236213.
- [12] A. Jörgen Bakker, S. L. Brouwers, M. van der Stelt, and dr C. ir Slump J de Witte, “MANUAL-UPPER LIMB PROSTHESES & COVERS,” 2022.
- [13] W. Brink, “3DTR Supporting Documentation”.
- [14] W. Zeiler, *Basisboek. Ontwerpen. Van Methodisch Ontwerpen tot Integraal Ontwerpen*, Eerste Druk. Noordhoff Uitgevers bv, 2014.
- [15] A. Chadwell *et al.*, “Technology for monitoring everyday prosthesis use: a systematic review,” *J Neuroeng Rehabil*, vol. 17, no. 1, p. 93, Dec. 2020, doi: 10.1186/s12984-020-00711-4.

- [16] T. J. Bates, J. R. Ferguson, and S. N. Pierrie, "Technological Advances in Prosthesis Design and Rehabilitation Following Upper Extremity Limb Loss," *Curr Rev Musculoskelet Med*, vol. 13, no. 4, pp. 485–493, Aug. 2020, doi: 10.1007/s12178-020-09656-6.
- [17] E. Biddiss, D. Beaton, and T. Chau, "Consumer design priorities for upper limb prosthetics," *Disabil Rehabil Assist Technol*, vol. 2, no. 6, pp. 346–357, Jan. 2007, doi: 10.1080/17483100701714733.
- [18] P. J. Kyberd, D. J. Dp. Beard, J. J. Davey, and J. D. Morrison, "A Survey of Upper-Limb Prosthesis Users in Oxfordshire," *JPO Journal of Prosthetics and Orthotics*, vol. 10, no. 4, pp. 84–91, 1998.
- [19] J. Barrios-Muriel, F. Romero-Sánchez, F. J. Alonso-Sánchez, and D. Rodríguez Salgado, "Advances in Orthotic and Prosthetic Manufacturing: A Technology Review," *Materials*, vol. 13, no. 2, p. 295, Jan. 2020, doi: 10.3390/ma13020295.
- [20] C. Nayak, A. Singh, and H. Chaudhary, "Customised prosthetic socket fabrication using 3D scanning and printing," 2014. [Online]. Available: <https://www.researchgate.net/publication/274386505>
- [21] G. Colombo, C. Rizzi, D. Regazzoni, and A. Vitali, "3D interactive environment for the design of medical devices," *International Journal on Interactive Design and Manufacturing (IJIDeM)*, vol. 12, Oct. 2018, doi: 10.1007/s12008-018-0458-8.
- [22] M. Karakoç, İ. Batmaz, M. A. Sariyildiz, L. Yazmalar, A. Aydin, and S. Em, "Sockets Manufactured by CAD/CAM Method Have Positive Effects on the Quality of Life of Patients With Transtibial Amputation," *Am J Phys Med Rehabil*, vol. 96, no. 8, pp. 578–581, Aug. 2017, doi: 10.1097/PHM.0000000000000689.
- [23] N. Herbert, D. Simpson, W. D. Spence, and W. Ion, "A preliminary investigation into the development of 3-D printing of prosthetic sockets," *The Journal of Rehabilitation Research and Development*, vol. 42, no. 2, p. 141, 2005, doi: 10.1682/JRRD.2004.08.0134.
- [24] J. Allum, A. Moetazedian, A. Gleadall, and V. V. Silberschmidt, "Interlayer bonding has bulk-material strength in extrusion additive manufacturing: New understanding of anisotropy," *Addit Manuf*, vol. 34, p. 101297, Aug. 2020, doi: 10.1016/j.addma.2020.101297.
- [25] J. C. H. Goh, P. V. S. Lee, and P. Ng, "Structural integrity of polypropylene prosthetic sockets manufactured using the polymer deposition technique," *Proc Inst Mech Eng H*, vol. 216, no. 6, pp. 359–368, Jun. 2002, doi: 10.1243/095441102321032157.
- [26] P. Maroti *et al.*, "Printing orientation defines anisotropic mechanical properties in additive manufacturing of upper limb prosthetics," *Mater Res Express*, vol. 6, no. 3, p. 035403, Dec. 2018, doi: 10.1088/2053-1591/aaf5a9.
- [27] B. Pousett, A. Lizcano, and S. U. Raschke, "AN INVESTIGATION OF THE STRUCTURAL STRENGTH OF TRANSTIBIAL SOCKETS FABRICATED USING CONVENTIONAL METHODS AND RAPID PROTOTYPING TECHNIQUES," *Canadian Prosthetics & Orthotics Journal*, Apr. 2019, doi: 10.33137/cpoj.v2i1.31008.
- [28] B. Redwood, F. Schöffner, and B. Garret, *The 3D Printing Handbook*. 2017.
- [29] O. H. Ezeh and L. Susmel, "On the fatigue strength of 3D-printed polylactide (PLA)," *Procedia Structural Integrity*, vol. 9, pp. 29–36, 2018, doi: 10.1016/j.prostr.2018.06.007.

- [30] Fillauer TRS Inc, "Omega Wrist." Accessed: Mar. 18, 2023. [Online]. Available: <https://www.trsprothetics.com/product/omeg-wrist/>
- [31] D. W. Abbot, D. V. V. Kallon, C. Anghel, and P. Dube, "Finite Element Analysis of 3D Printed Model via Compression Tests," *Procedia Manuf*, vol. 35, pp. 164–173, 2019, doi: 10.1016/j.promfg.2019.06.001.

## Appendix

### Appendix A: Program of Requirements

Functional requirements	Code	Requirement	Source	Fixed	Variable
Assembly	Fu - As 1	The prosthetic device allows the local prosthetic maker to assemble the prosthetic device in less than 10 steps	3DSL		
Assembly	Fu - As 2	The prosthetic device allows the patient to assemble the prosthetic device in less than 10 steps	3DSL		
Assembly	Fu - As 3	The connection methods allow for one-handed assembly	Masanga Hospital		
Modulair	Fu - Mo 1	The adapters (hands, hooks, etc.) can be placed in different positions by the local prosthetic maker, allowing for more pronation and supination	Masanga Hospital		
Modulair	Fu - Mo 2	The adapters (hands, hooks, etc.) can be placed in different positions by the patient, allowing for more pronation and supination	Masanga Hospital		
Modulair	Fu - Mo 3	The prosthetic device supports interchangeable adapters (hands, hooks, etc.) that can be seamlessly attached and detached from the arm	Masanga Hospital		
Modulair	Fu - Mo 4	The connections above and below the elbow module of the transhumeral prosthetic device is modular, allowing for interchangeability of components	Masanga Hospital		
Strength	Fu - St 1	The connections does not contain unwanted movement or disconnection during use.	3DSL		
Strength	Fu - St 2	The connection can withstand the forces of lifting a 98.1 N load horizontally	Masanga Hospital		

Fabrication requirements	Code	Requirement	Source	Fixed	Variable
Appearance	Fa - Ap 1	The prosthetic device will exhibit a high degree of anatomical resemblance	Masanga Hospital		
Costs	Fa - Co 1	The connection methods are designed with cost-effectiveness in mind to keep the costs of the prosthetic devices below 30 euros	3DSL		
Durability	Fa - Du 1	The connections are able to withstand repetitive use over an extended period without experiencing significant wear or degradation	Masanga Hospital		
Durability	Fa - Du 2	The connections are able to withstand an environment containing 100% humidity	3DSL		
Durability	Fa - Du 3	The connections are able to withstand an environment containing temperatures of 40°C	3DSL		
Realization	Fa - Re 1	The connection methods are standardized	3DSL		
Realization	Fa - Re 2	The prosthetic device is compatible with 3D printing technology	3DSL		
Weight	Fa - We 1	The weight of the prosthetic device with the connection methods does not exceed 1,5 kg	Masanga Hospital		
Weight	Fa - We 2	The positioning of the hand minimizes the need for support structures during the printing process	3DSL		

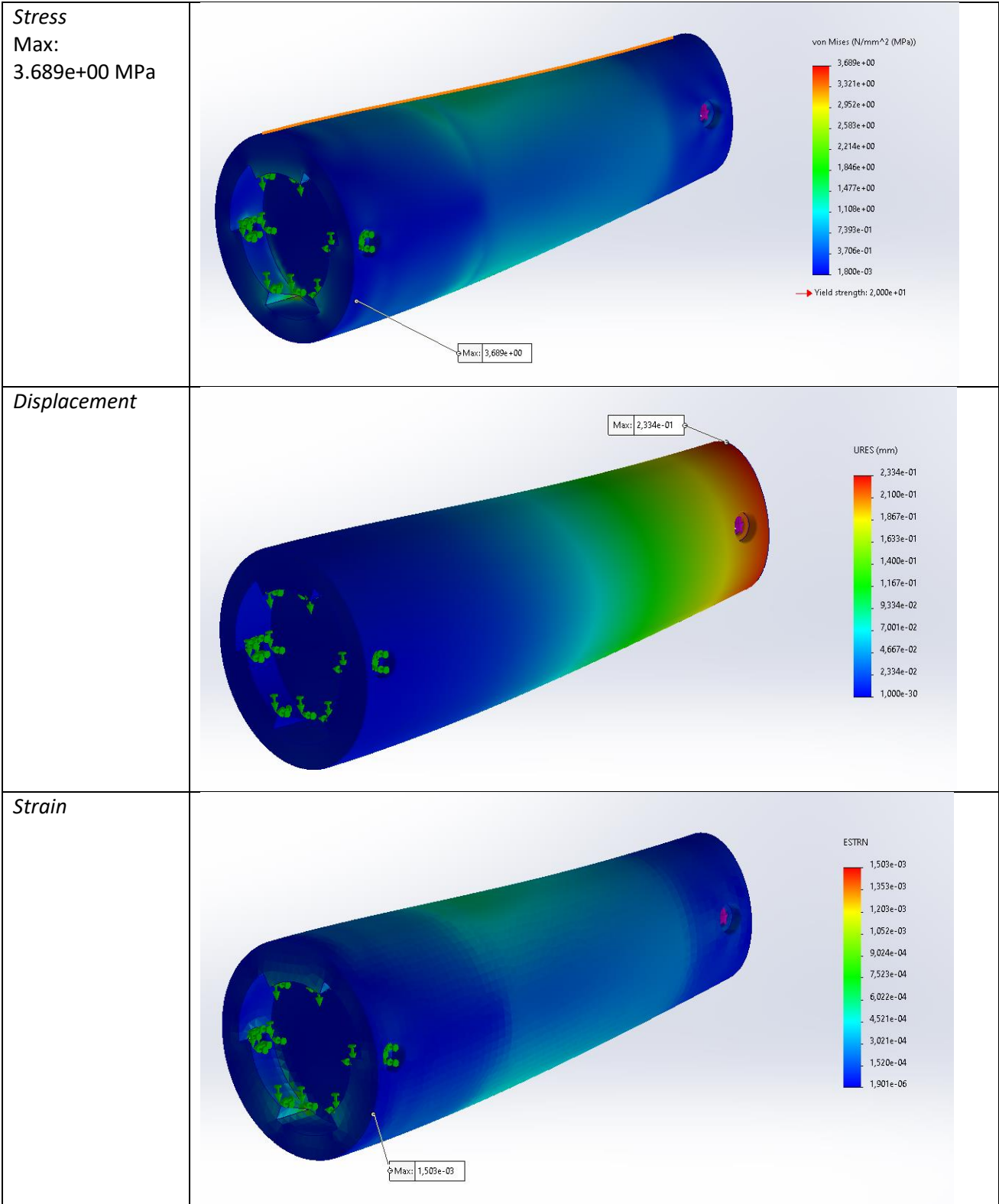
Appendix B: Morphological Overview Selected

Function	Method 1	Method 2	Method 3	Method 4	Method 5	Method 6	Method 7
Connection in the wrist	Bayonet 	Thread 	Omega 	Pyramid Adapter 	Clamped 	Quick Lock Pin 	
Additional connection method	Bolt and nut 	Set screw 	None 				
Change position hand/adapter	Bayonet 	Thread 	Omega 	Pyramid Adapter 	Spherical Joint 	Clamped 	Fixed Slots 
Connection below elbow (transhumeral)	Bayonet 	Thread 	Bolted 	Omega 	Clamped 	Set Screw 	
Connection above elbow (transhumeral)	Bayonet 	Thread 	Bolted 	Omega 	Clamped 	Set Screw 	
Concepts	I	II	III	IV	V	VI	



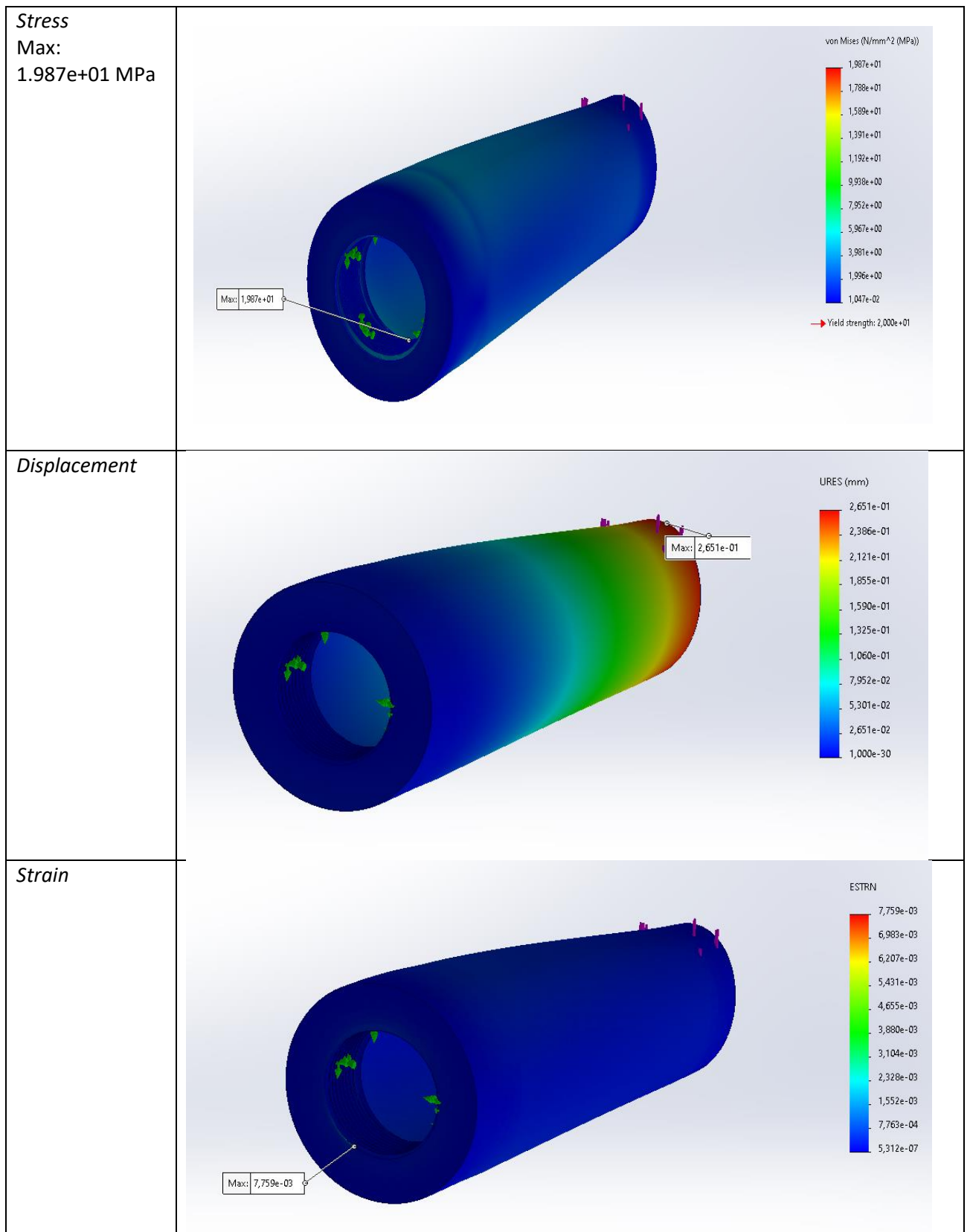
Appendix C: FEA for the Concepts

Concept 1: Bayonet

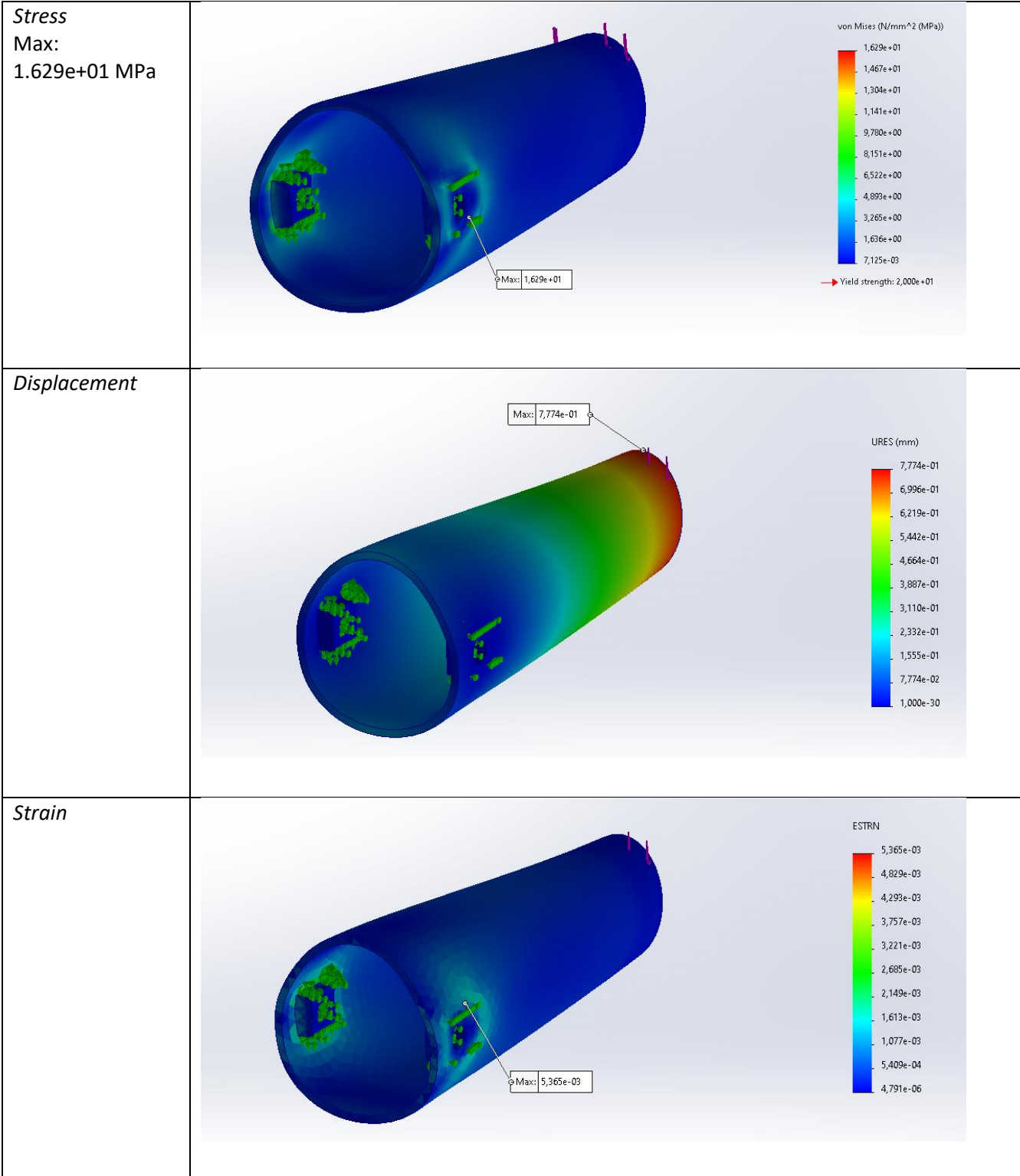




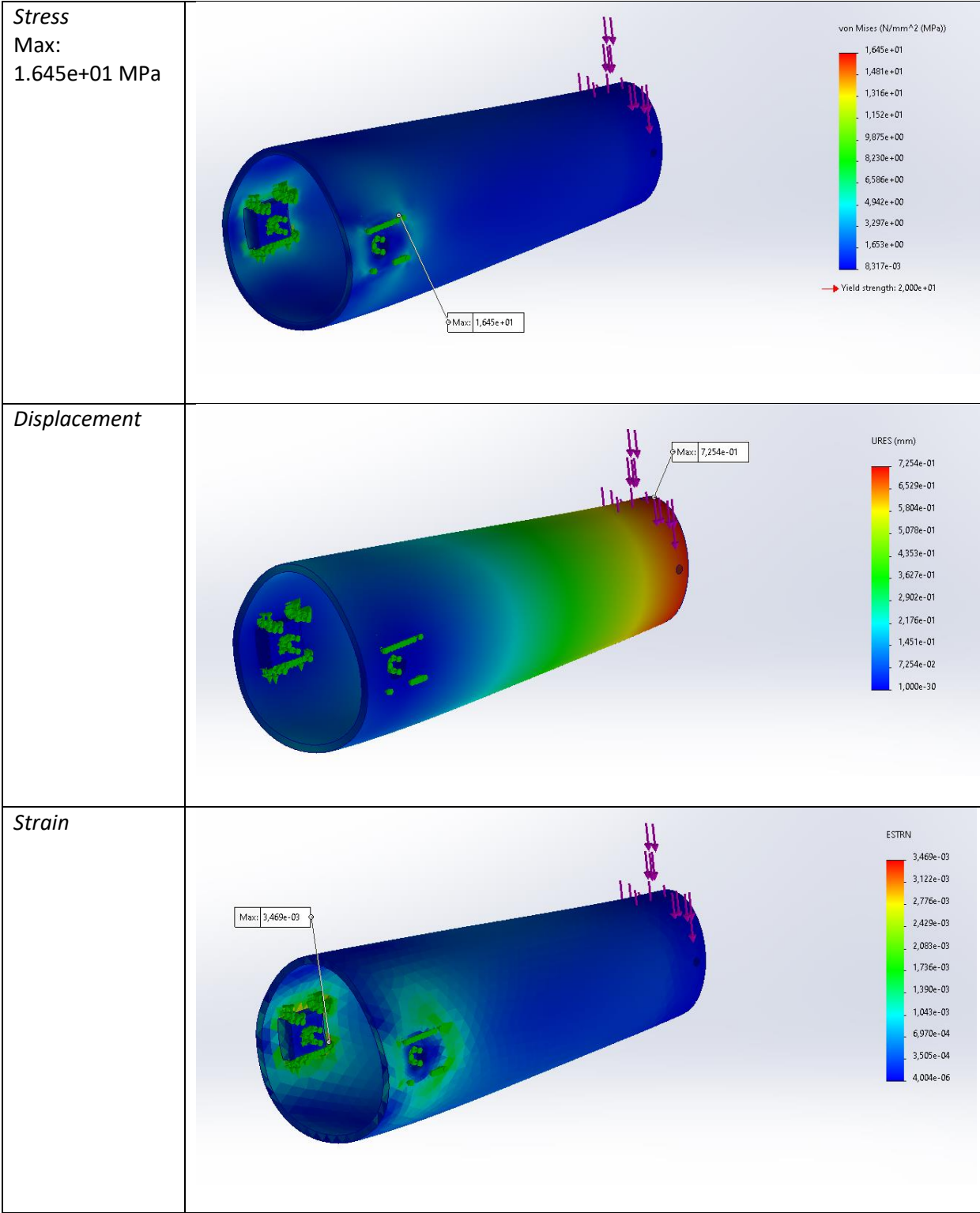
## Concept 2: Threaded



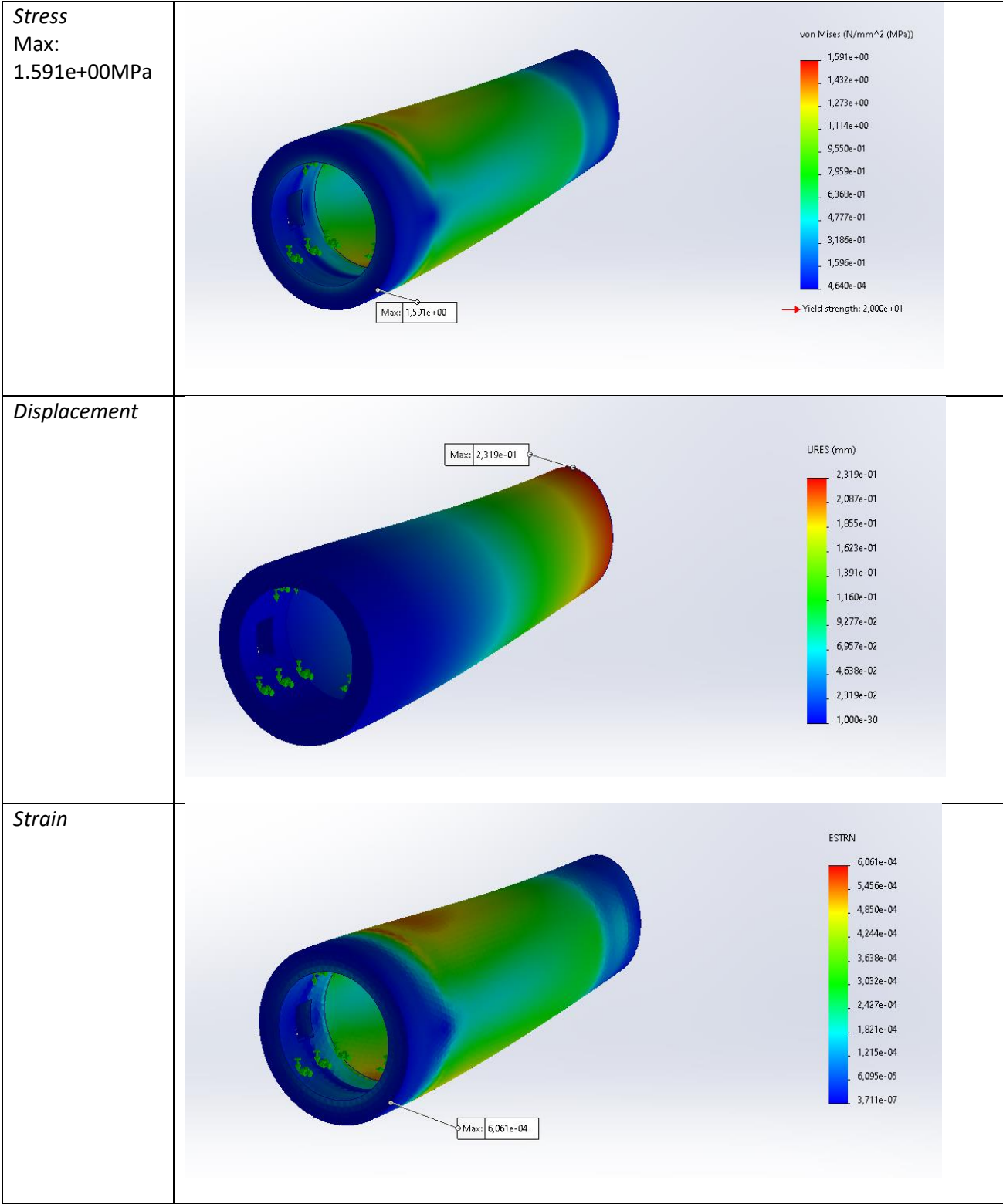
**Concept 3: Omega**



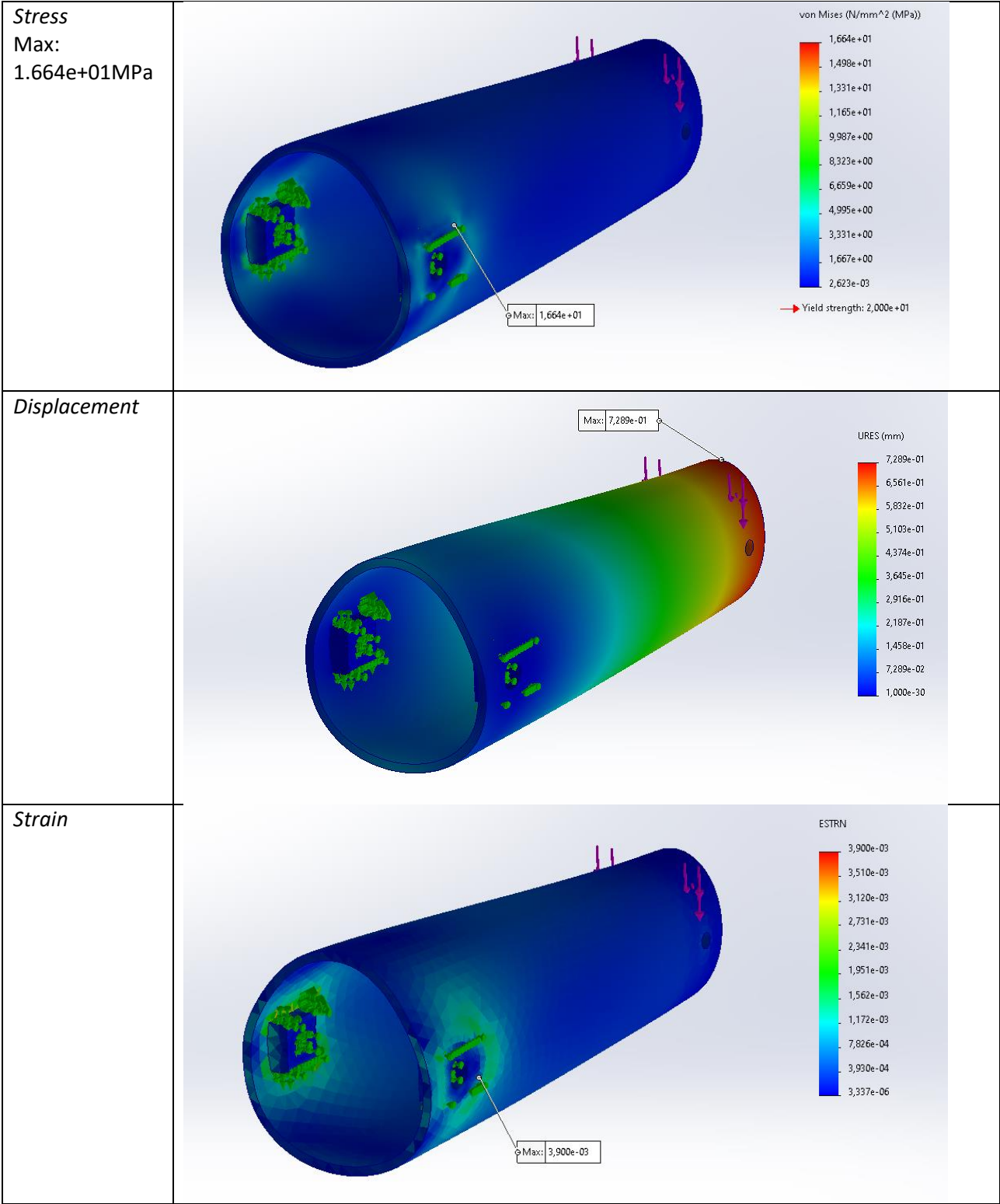
**Concept 4: Pyramid**



**Concept 5: Clamped**



**Concept 6: Quick Lock Pin**



## Appendix D: Scoring Tables

### Functional scoring

Code	Concept I	Concept II	Concept III	Concept IV	Concept V	Concept VI	Ideal
<i>Fu - As 2</i>	1	9	5	2	4	5	<b>12</b>
<i>Fu - As 3</i>	8	14	11	2	10	10	<b>16</b>
Total	9	23	16	4	14	15	<b>28</b>
Percentage %	32.143	82.143	57.143	14.286	50.000	53.571	<b>100</b>

### Fabrication scoring

Code	Concept I	Concept II	Concept III	Concept IV	Concept V	Concept VI	Ideal
<i>Fa - Co 1</i>	5	7	6	2	2	4	<b>8</b>
<i>Fa - Re 2</i>	9	11	10	6	9	9	<b>12</b>
<i>Fa - We 1</i>	5	7	6	2	5	5	<b>8</b>
<i>Fa - We 2</i>	2	2	2	2	3	2	<b>4</b>
Total	21	27	24	12	19	20	<b>32</b>
Percentage %	65.625	84.375	75.000	37.500	59.375	62.500	<b>100</b>

### Overall scoring

Code	Concept I	Concept II	Concept III	Concept IV	Concept V	Concept VI	Ideal
<i>Fu</i>	9	23	16	4	14	15	<b>28</b>
<i>Fa</i>	21	27	24	12	19	20	<b>32</b>
Total	30	50	40	16	33	35	<b>60</b>
Percentage %	50.000	83.333	66.667	26.667	55.000	58.333	<b>100</b>



## Appendix E: Iterative Steps

### Appendix E.1. Iterative Steps - Threaded Concept

#### Iterative Development

##### *Elbow module connection*

Initially, a pitch of 2 mm was employed. This proved to be working near the yield stress region when a load of 100 N was applied, see Appendix C: FEA for the Concepts. To overcome this, the pitch was revised to 5 mm, ensuring greater durability and load-bearing capacity. This adjustment allowed the thread to withstand higher loads in the perpendicular axis, as the stresses in the proximal threaded part dropped significantly for the applied load of 100N, see Appendix G.1. Additional FEA - Threaded Concept.

The applied load was increased with 100N in the Y-axis (perpendicular to the wrist) until the stresses were just below the yield strength ( $2.000e+01$  MPa), see Table 8.

Furthermore, the thread configuration within the elbow module was optimized to function effectively without the need for an offset or fillet. The selected size measures 48x5 (diameter x pitch), demonstrating robust performance and reliability, see Figure 23.

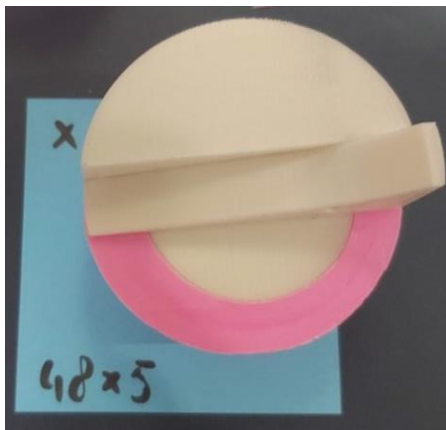


Figure 23 Best combination concept 2 proximal end forearm: no offset and no fillet for nut

Table 8 Applied loads on the adjusted forearm with corresponding stresses

Max. Stress [MPa] ->	Y
Applied Load	
100N	3.314e+00
200N	6.623e+00
300N	9.934e+00
400N	1.325e+01
500N	1.656e+01
600N	1.987e+01

##### *Wrist module connection*

Initially, a screw setup measuring 25x2 (diameter x pitch) was found to be excessively tight. Attempts to alleviate this tightness by introducing an additional leverage block proved ineffective.

Transitioning the screws with dimensions of 27x2 yielded similar tightness concerns, despite multiple attempts to mitigate the issue using an extra leverage block. Shifting to thread measurements of 27x3, without an offset, also failed to resolve the tightness problem. A refined solution emerged by introducing a subtle offset of -0.2mm for both the bolt (located at the adapter end of the hand) and the nut (inserted into the wrist of the forearm). This adjustment achieved good functionality, striking a delicate balance between tightness and looseness, offering a slight degree of play without compromising structural integrity. Further refinement was accomplished by incorporating a -0.2mm offset and a 0.25mm fillet for both the bolt and nut. This last configuration ensured a secure yet flexible fit. Additionally, the positioning of the screw configuration depended on various locations where a gap was implemented in the bolt's thread to accommodate an external screw. These fixed positions were replaced with a slot, enhancing adaptability and versatility within the design. Pictures of the iterative steps of the wrist for concept two can be found in Appendix F.1.

By combining the different bolts and nuts with different offsets and fillets, the best combination is obtained via visual inspection. The final configuration which works best is the combination of -0.2mm offset (-0.1mm offset on both sides of the thread) and a fillet of 0.25mm on the outside of the thread of the bolt, while no offset and no fillet is applied on the nut, see Figure 24.



Figure 24 Best combination concept 2: -0.2mm offset and 0.25mm fillet on thread with no offset and no fillet for nut

The static load analysis of a simplified version of the hand (75mm x 55mm x 135mm) with the corresponding adapter can be found in Appendix G.1.

### Concept Evaluation

The current method employed for the connections on both sides of the forearm demonstrates effectiveness in many aspects. However, a significant bottleneck emerges due to the necessity of using a screw within this configuration. This bottleneck primarily relates to the challenges associated with utilizing a metal screw within a plastic component.

A major concern is the damage to the plastic component. The interaction of metal screws with plastic components can lead to various issues, including the risk of structural damage, see Figure 25. This encompasses scenarios where the threads within the plastic may be stripped or otherwise compromised due to the use of metal screws. Such wear and tear over time can have adverse effects on the integrity of the connection, necessitating maintenance or replacements, which in turn result in additional costs.

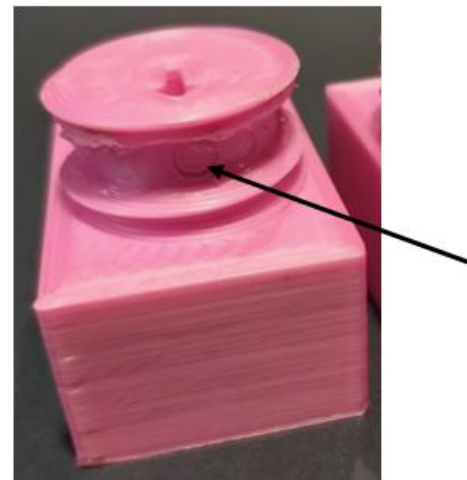


Figure 25 Slot of the threaded part showing the damages of a metal screw

## Appendix E.2. Iterative Steps - Omega Concept

### Iterative Development

#### Elbow module connection

The utilization of a bolt and nut configuration proves effective in ensuring a secure connection. However, it is important to note that over-tightening this connection can result in deformation of the forearm around the elbow module, consequently elevating internal stresses within the forearm shell. Furthermore, physical testing indicated that operating this connection method with one hand poses a challenge. In response to these issues, a solution is sought by increasing the parts of the lower elbow module that are in contact with the forearm as highlighted with circles in Figure 26. The static analysis of the forearm of this concept can be found in Appendix G.2. Additional FEA - Omega Concept.

#### Wrist module connection

The distal part of the forearm for the wrist module is 3D-printed including the guidance and the adapter to check if the method works, see Appendix F.2. for corresponding iteration pictures of the forearm wrist module. The guidance was printed with a height of 5 mm, but this was found to be too small to withstand the applied stresses. To overcome this, the same thread settings used in concept 2 were implemented (diameter x pitch = 27x3, height = 10mm, offset = -0.2mm and fillet = 0.25mm; with zero offset and fillet for the internal thread in the forearm). This configuration proved effective. The guidance was printed with both a 0.8mm and 0.4mm nozzle. The 0.4mm nozzle proved to be best suitable for the printing of the guidance as the resolution of the threads using the 0.8mm nozzle did not allow for smooth operation of the threads. The next step in the development process for this concept was the exploration of the omega-shaped spring design for gripping onto the adapter. Using the prototype for proving the working of this concept, it was found that the omega-shaped spring would not be able in this small proportion. For this, a metallic wire had to be placed around the shaft as well as the purchase of two metallic springs. All these compartments would be applying forces on plastic parts which would degrade the lifetime drastically, as seen in the threaded part with the set screw of concept 2. To solve this problem, another method was implemented for this: 3D-printed torsion springs.

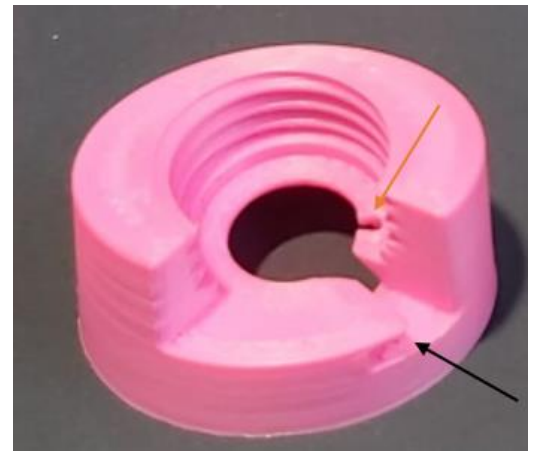


Figure 27 Third iteration wrist module with 1/3 removed for internal observation. Increased height for guidance, added hole as an anchor point for torsion spring (brown arrow), small edge of 2.2mm for locked position (black arrow).

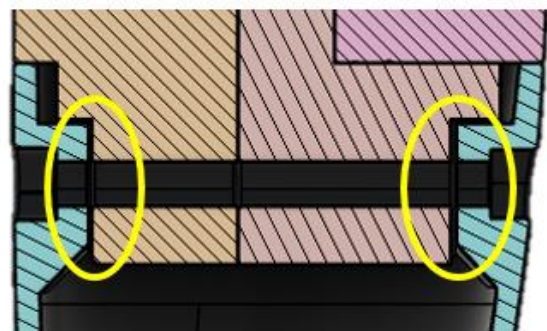
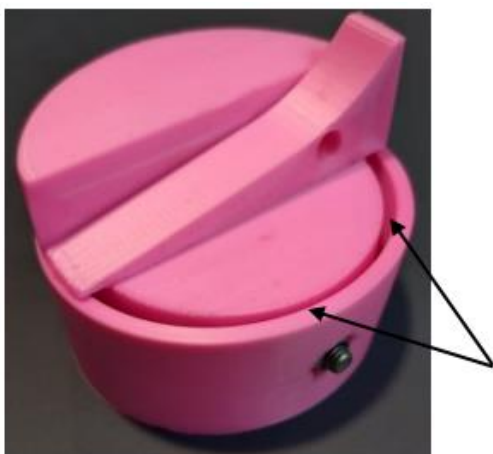


Figure 26 Left: Bolted connection proximal end forearm. The black arrow indicates the differences in deformation due to overtightening.

Right: Lower part of elbow module which highlights the adjusted parts to reduce overtightening of the screw.

The first observation made during this phase was that increasing the revolutions (more than 1) of the spring did not yield the desired results of gripping onto the shaft when operating the torsion spring. Instead, it led to an undesirable increase in width, particularly concerning the central circular component that should be tightened. To address this, the revolutions were decreased to a maximum of 1.0, and additional modifications were made to enhance the functionality. One of these modifications is adding an anchor point for the torsion spring to rotate around. This ensures the torsion spring will be wrapped around the shaft better when the torsion spring is closed.

For the new iteration of the distal part of the forearm, approximately one-third of the front part of the design was intentionally removed to gain insight into the internal mechanics and to make necessary adjustments, as illustrated in Figure 27 for the third iteration. These adjustments encompassed several key aspects. An increase in the height of the guidance and the overall range for the torsion spring was made to accommodate the torsion spring effectively. The length of the guidance part is extended from 5mm to 10 mm, drawing inspiration from the threaded adapter of Concept 2. Furthermore, an anchor point was introduced to secure one end of the torsion spring, ensuring its stability within the design, see the brown arrow in Figure 30.

The next evolution of the torsion spring design involved the use of a revolution setting of 0.5 (equivalent to 1 pi). However, this configuration proved to be too tight, leading to the breaking of the lever component, and the absence of a suitable locking mechanism for the lever. Nevertheless, this iteration allowed for testing of the locking mechanics of the adapter, which proved to be successful. One challenge encountered in this phase was the difficulty in inserting the adapter into the device due to interference from the spring as the spring did not have enough room to open completely.

The realization that the outer end of the torsion spring needed to be clamped when locking the adapter led to further refinements. For the third iteration of the wrist module, a small edge of 2.2 mm was added for the spring to securely clamp behind, see black arrow in Figure 27. The 2.2 mm is found during testing with the previous iteration for enough space for the torsion spring pin. The range of motion for the spring was reduced to minimize the risk of breakage while maintaining sufficient space for ease of adapter and hand attachment to the wrist. The subsequent torsion spring design iteration featured a revolution setting of 0.7 (equivalent to 1.4 pi). This setting allowed for the expansion of the spring, facilitating the insertion of the adapter into the insert. Despite this improvement, occasional breakages of the lever were observed, see Figure 28. To address this issue, enhancements were made, including the introduction of chamfers and eventually chamfers combined with fillets. Since these adjustments, the lever has remained intact. Another finding during this phase was the continuous return of the blob in the anchor pin, see the black arrow in Figure 28. This resulted in additional post-processing steps to fit the anchor point in the forearm, see the brown arrow in Figure 27.



*Figure 28 Torsion spring with width 2mm, 15mm diameter and 0.7 revolutions which broke due to overstressing the lever. The black arrow highlights the blob which occurs during printing with 0.4mm and 0.8mm nozzle.*

The design was further improved by closing a gap to replicate real-world wrist conditions. This adjustment enabled testing to confirm whether the torsion spring could be appropriately situated within the final wrist design. The overhanging part in the gap was omitted due to infeasibility, resulting in a smaller clamping cavity. During the testing phase, the design's printability was assessed in terms of bridging for the overhang, along with the identification of optimal locations for locking mechanisms to secure the gripping part on the adapter when engaged. Testing with the locking of

the torsion spring noticed the spring kept unlocking itself when a slight force was applied to the adapter.

The exploration of various scenarios for the torsion spring took place. Larger revolutions were employed for both 2mm and 3mm widths, using a 0.25mm nozzle. Additionally, the diameters were decreased to 10 mm and 8 mm, respectively, for testing. Both configurations resulted in component failure along adhesive lines. The width of 3 mm reduced the flexibility of the torsion spring. The 0.25mm nozzle did not introduce the typical blob that required manual removal when the spring was printed using a 0.4mm or 0.8mm nozzle, see black arrow in Figure 28. However, due to the easy breaking of the springs, the torsion spring was best to be printed with 0.8mm nozzle for a width of 2mm and 15mm diameter.

The final torsion spring design iteration adopted a revolution setting of 0.9 (equivalent to 1.8 pi). In this configuration, the device remains locked in a resting position, reducing ongoing stresses on the spring when the adapter is in place. The diameter of the torsion spring within the adapter's cavity was adjusted from 15mm to 11mm. To enhance the reliability of the torsion spring, limitations on the freedom of movement for the spring were decreased in the wrist module slide, minimizing the risk of excessive spring opening and potential breakage.

A new iteration of the locking mechanism was the implementation of slightly moving downwards when the pin moves to the right, after which it jumps upwards to be locked in place. The sliding part towards the lower right was too tight for smoothly operating the pin. This required lots of sanding and the supports were hard to remove in this tight area. Some parts which were interfering with the locking pin were manually removed to let the torsion spring move freely.

To address these problems, the next version contained an enlargement of the sliding parts to enhance functionality, as well as the removal of interfering components. The addition of a small slot to the left was made, which was intended to facilitate locking the spring in an open position for easier one-handed assembly and disassembly.

Eventually, the pin did still not move smoothly. To overcome this, the slide part was enlarged even more in the final iteration. The pin did not stay locked as planned in open position which resulted in an even larger slot for the pin to lock after, see black arrow in Figure 29.

The static load analysis of a simplified version of the hand (75mm x 55mm x 135mm) with the corresponding adapter can be found in Appendix G.2. Additional FEA - Omega Concept.

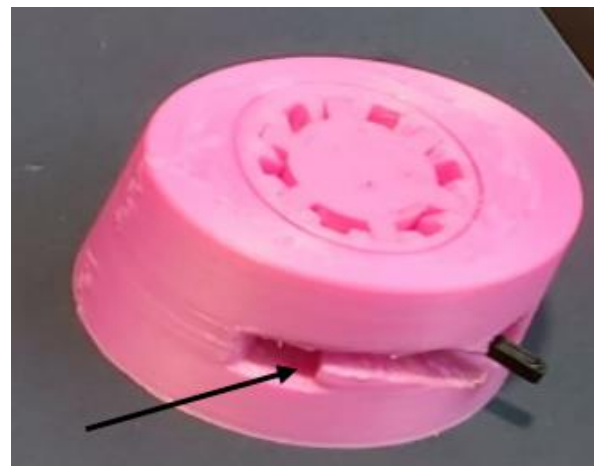


Figure 29 Final iteration of omega concept. Guidance, adapter and torsion spring are attached. The black arrow displays the gap after which the torsion pin is locked in the open position.



### Concept Evaluation

A notable strength of this concept lies in the ease of inserting, adapting the position, and removing the hand and its adapter. By applying the threads proved by the threaded concept, a reliable and secure connection mechanism is applied in the wrist module.

It is important to address the weakness of this design. As the thread in Concept 2 is wider than the adapter in this concept, it can be concluded that this connection method will be able to succumb under a lower load than Concept 2. Increasing the adapter in this concept will reduce the body between the thread and the wall of the forearm. This is unwanted as it will be able to cope with less loads.

The torsion spring is another weakness in the design, despite it being initially chosen for its functionality. It struggles to handle the stresses associated with opening and closing, which is a crucial aspect of its operation. This calls for a more robust spring or alternative locking mechanism to be implemented. Furthermore, the blob occurring during the 3D printing process is another area of concern. This unexpected occurrence necessitates additional post-processing steps to adjust, impacting the overall efficiency and production time.


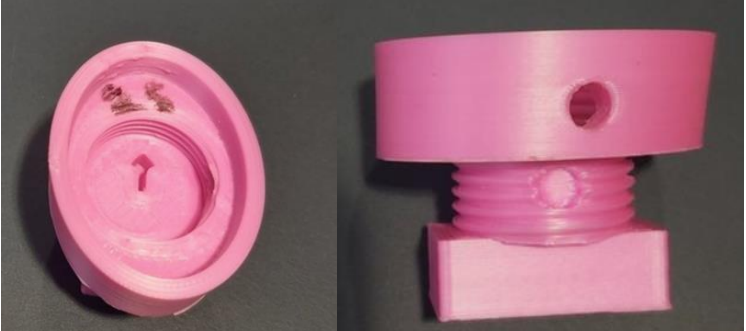
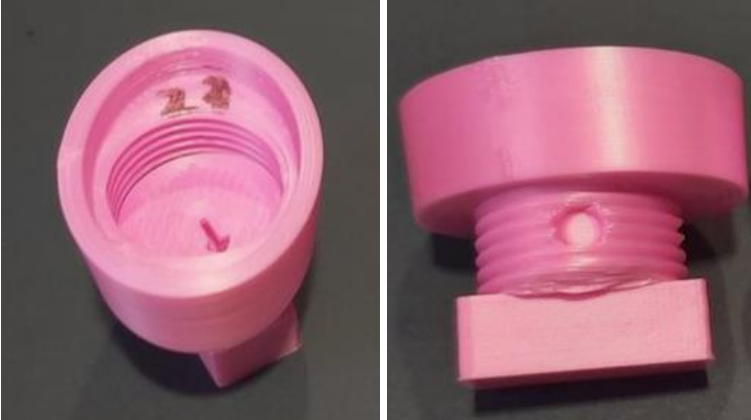
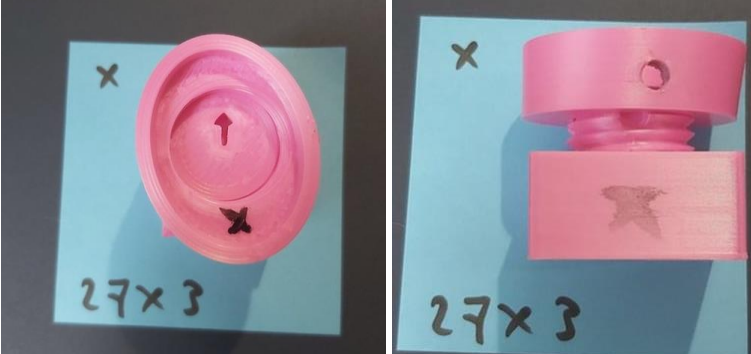


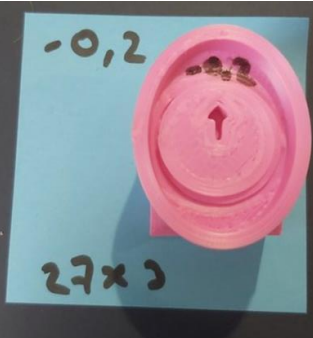
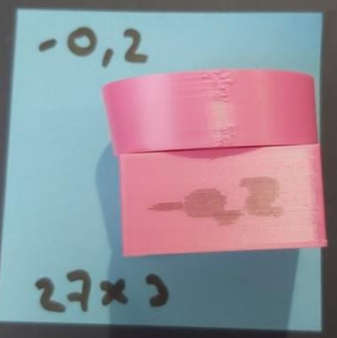
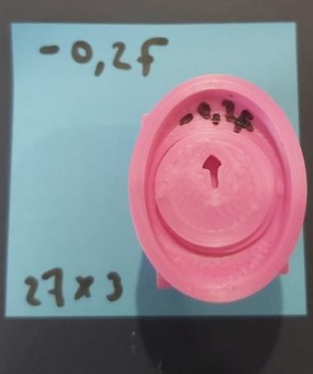


*Figure 30 Best combination for the wrist module of the omega concept.*







## Appendix F: Proof of Concepts




### Appendix F.1. Proof of Concepts - Threaded Concept

Adjustments	Pictures	
25x2		
25x2 additional block		
27x2		
27x3 The x indicates no offset and no fillet		

<p>27x3 -0.2 mm offset</p>			
<p>27x3 -0.2 mm offset +0.25 mm fillet</p>			
<p>Slot for thread containing -0.2 mm offset and 0.25 mm fillet</p>			

Appendix F.2. Proof of Concepts - Omega Concept

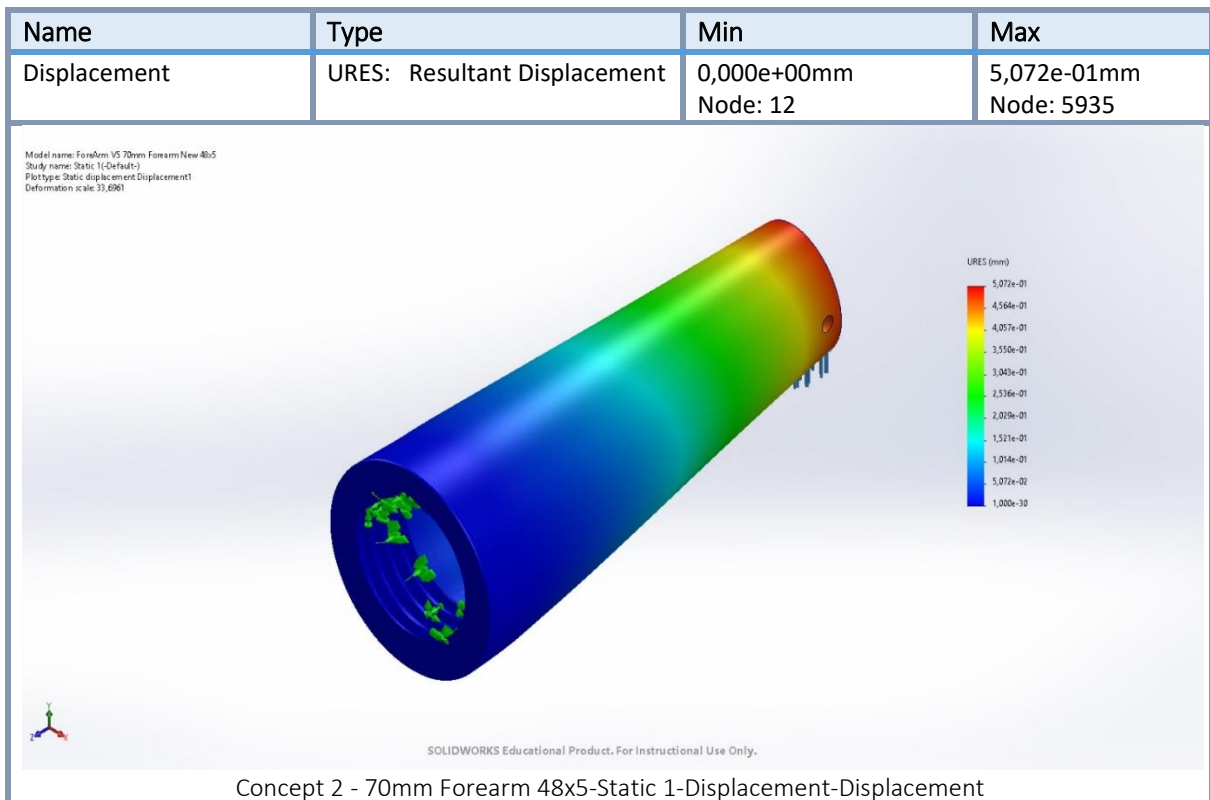
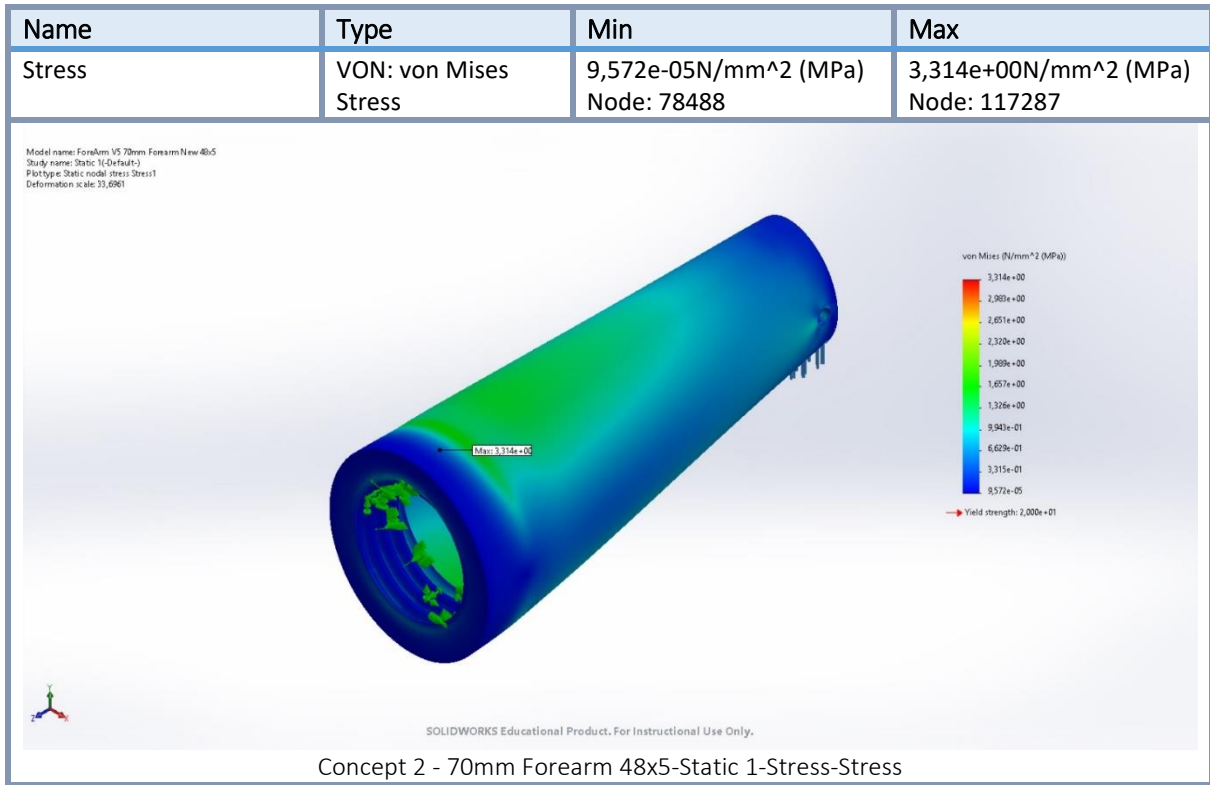
Adjustment	Pictures
Initial part	
Removed 1/3 to see the internal operations, height increased for the guidance (5 to 10 mm), anchor point added for torsion spring.	
Small edge added for the spring to clamp behind in closed position. Decreased range of motion for torsion spring.	
Closed the 1/3 part. Left out overhang.	

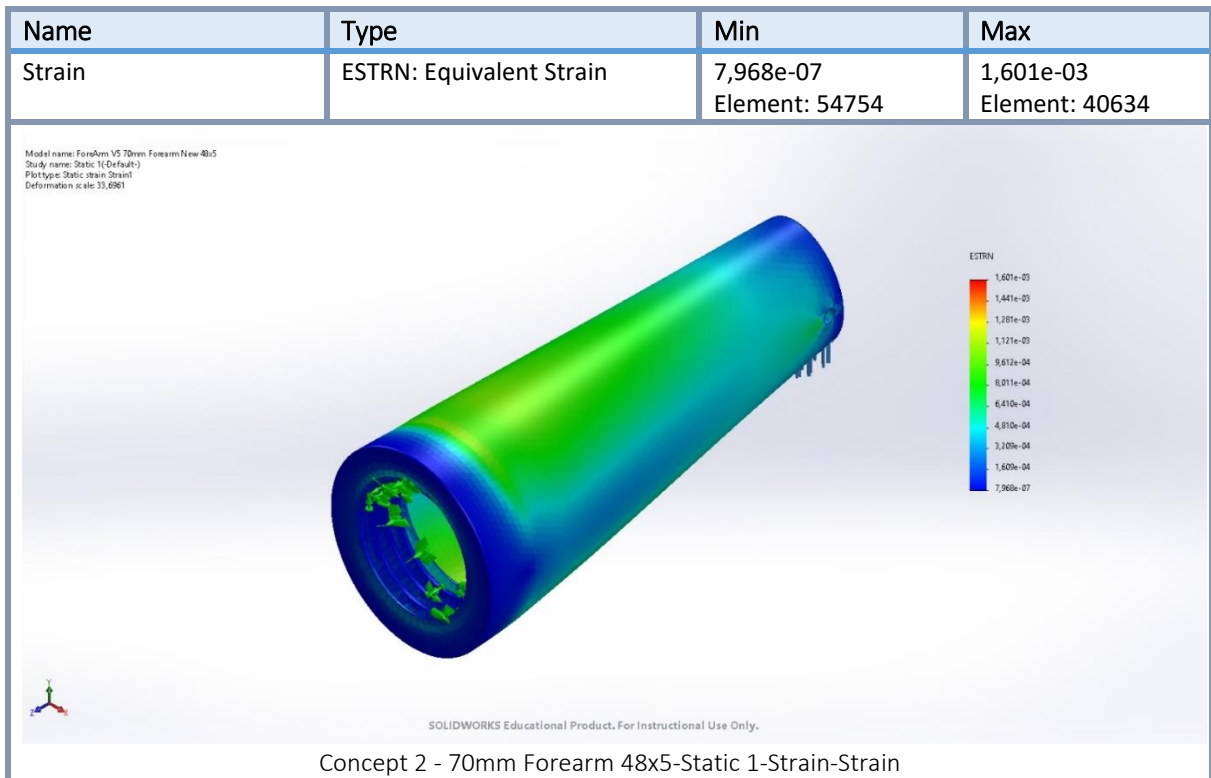
<p>Changed the locking mechanism for the torsion spring.</p>			
<p>Added the clamp mechanism to open the torsion spring.</p>			
<p>Increased the sliding part for smoother pin operation. Increased the locking part on the left for better locking when pin is opened.</p>			

## Appendix G: Additional FEA

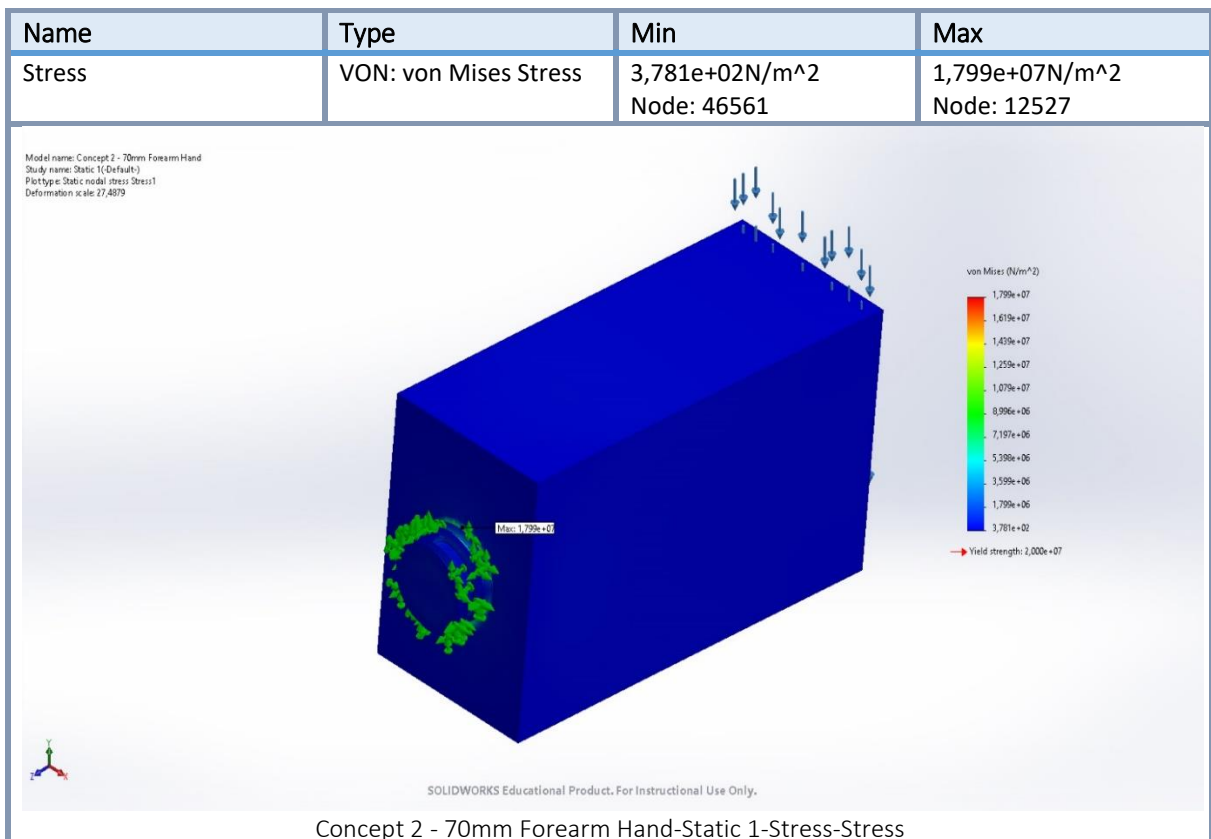
### Appendix G.1. Additional FEA - Threaded Concept

#### Forearm

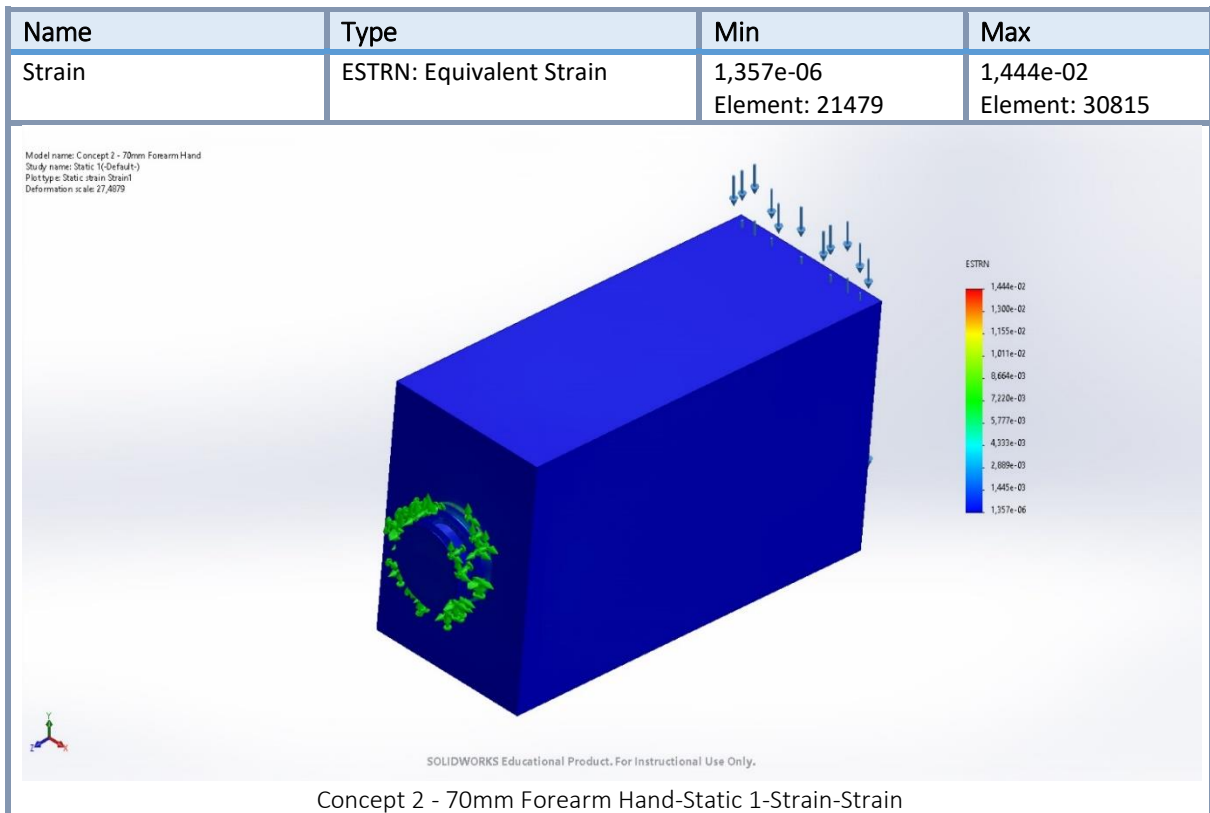
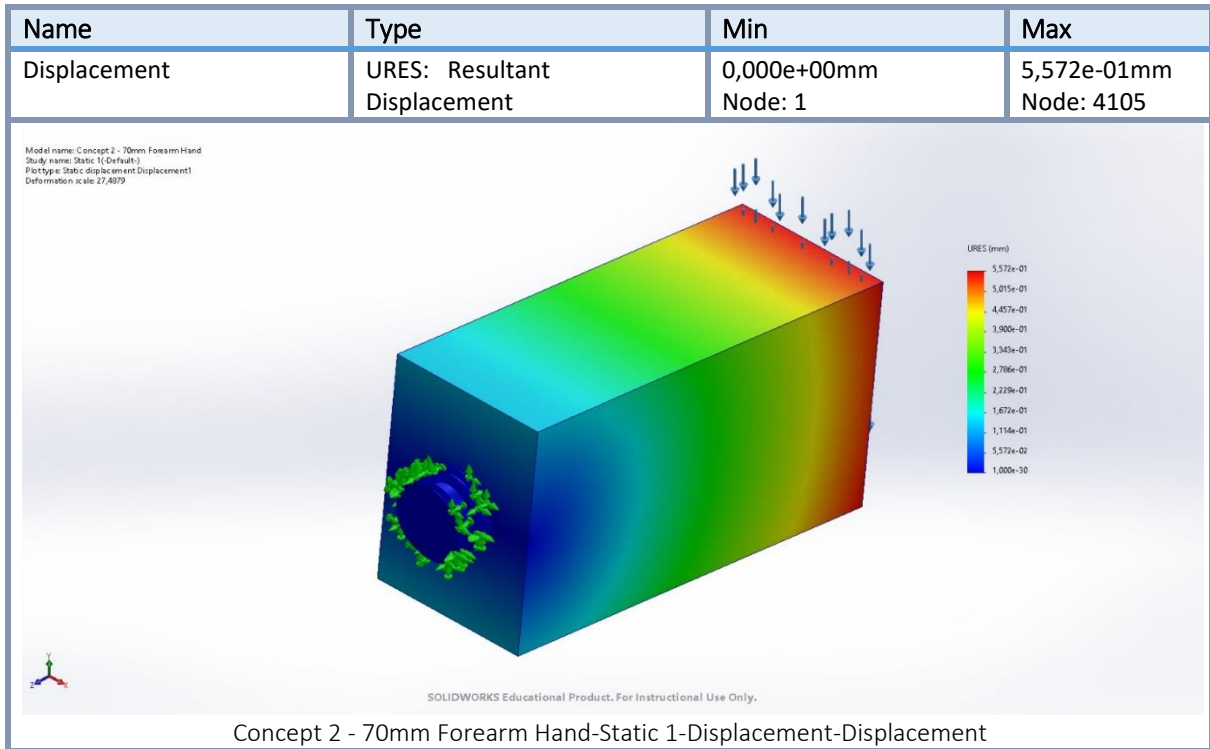




## Wrist

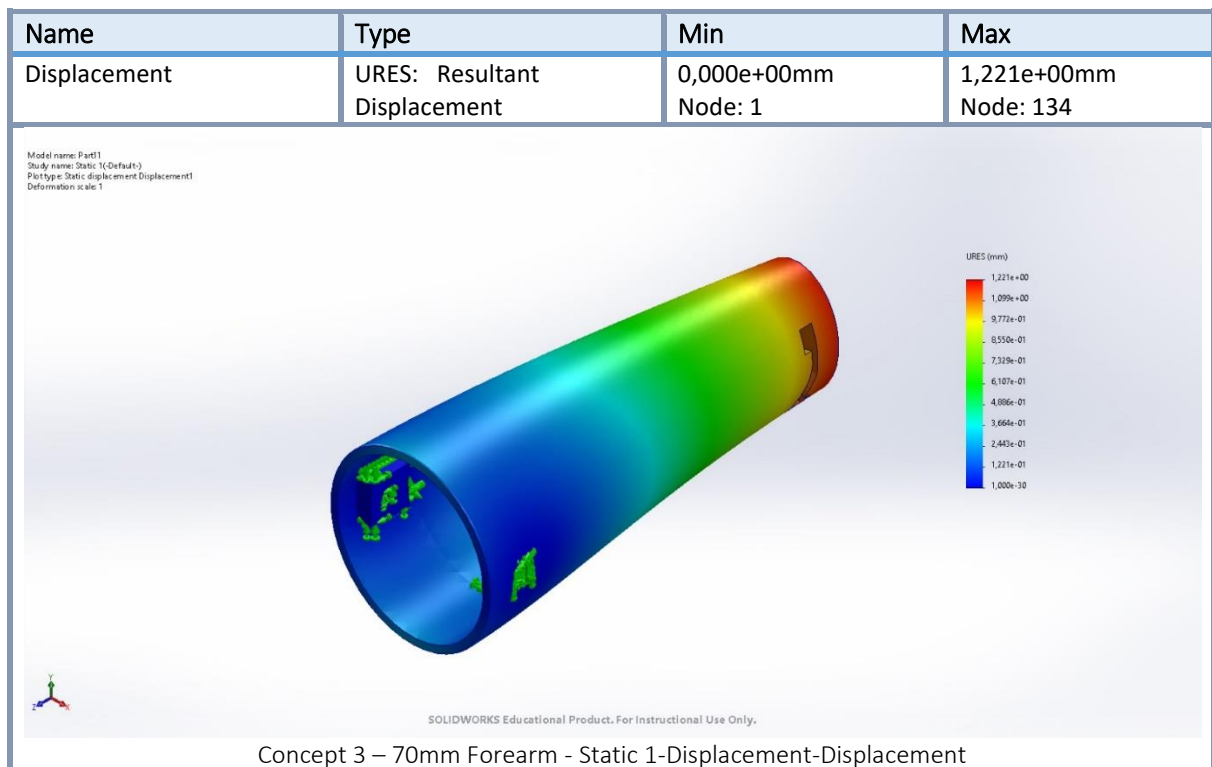
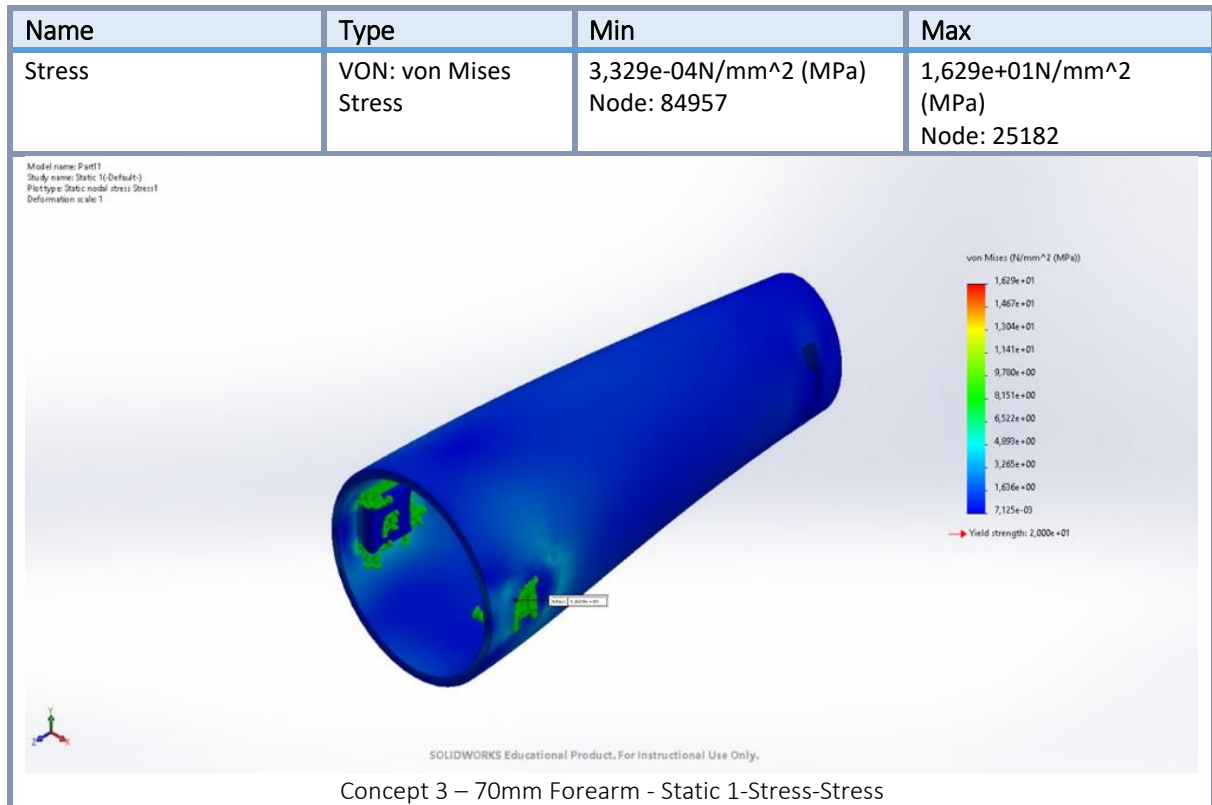


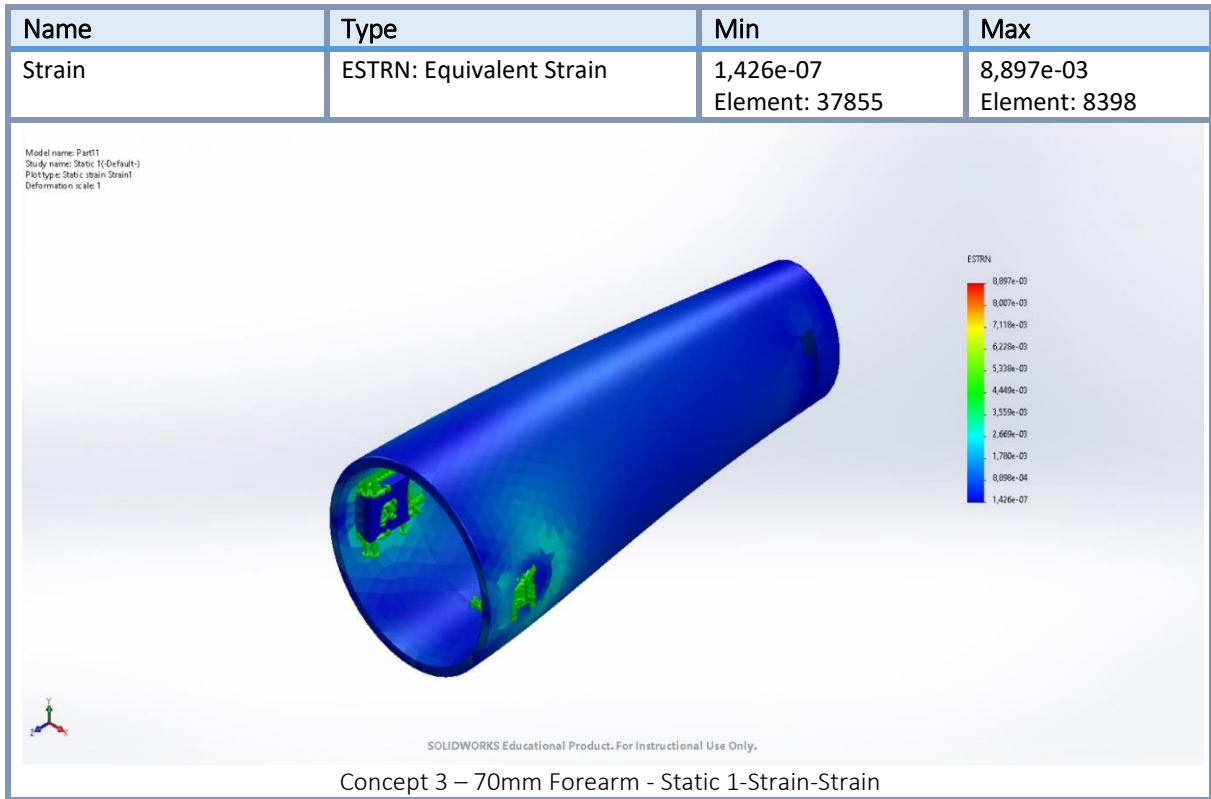




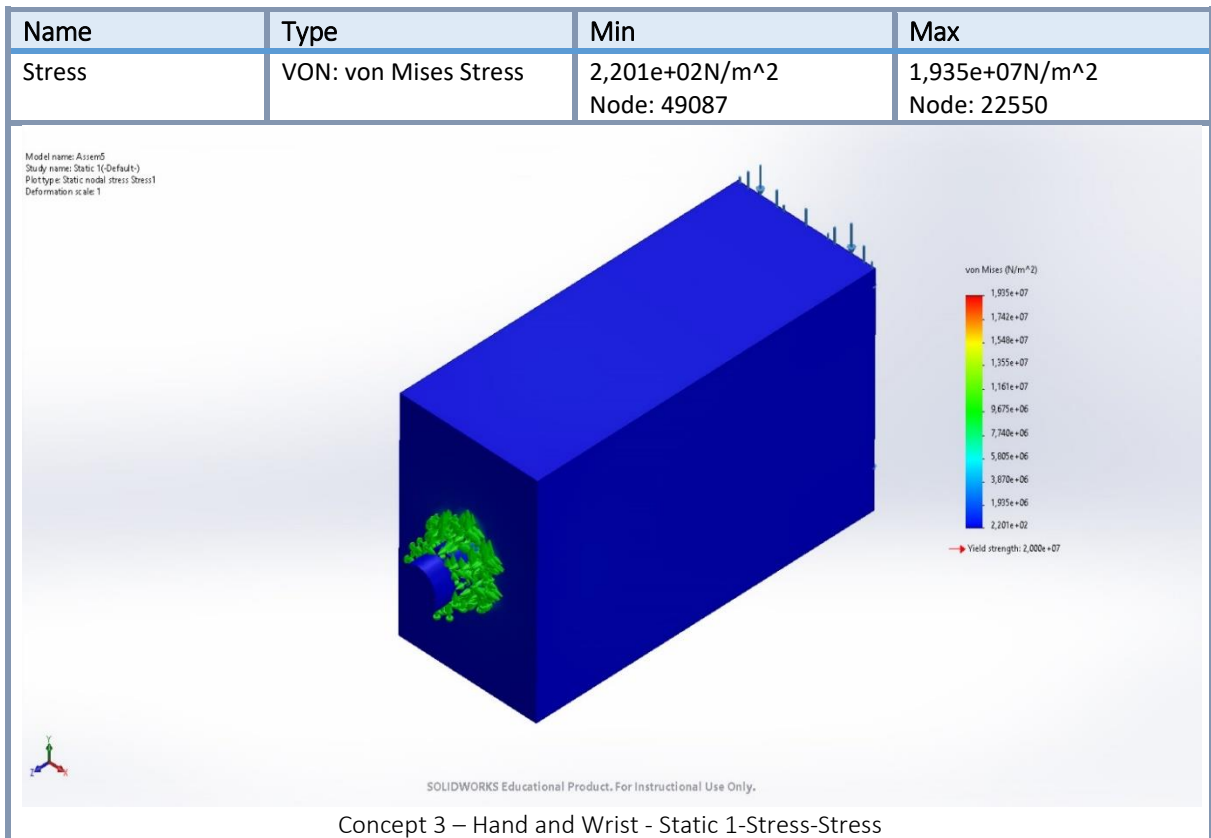
## Appendix G.2. Additional FEA - Omega Concept

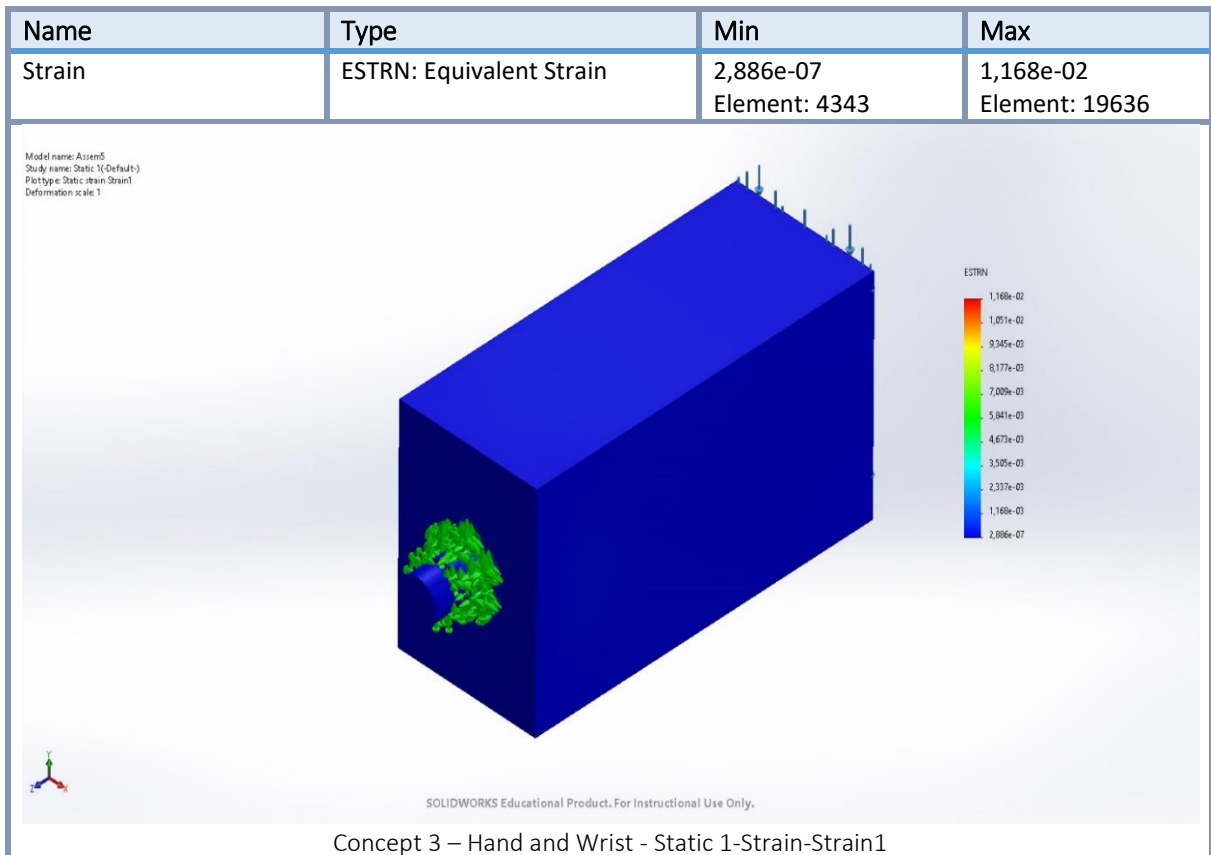
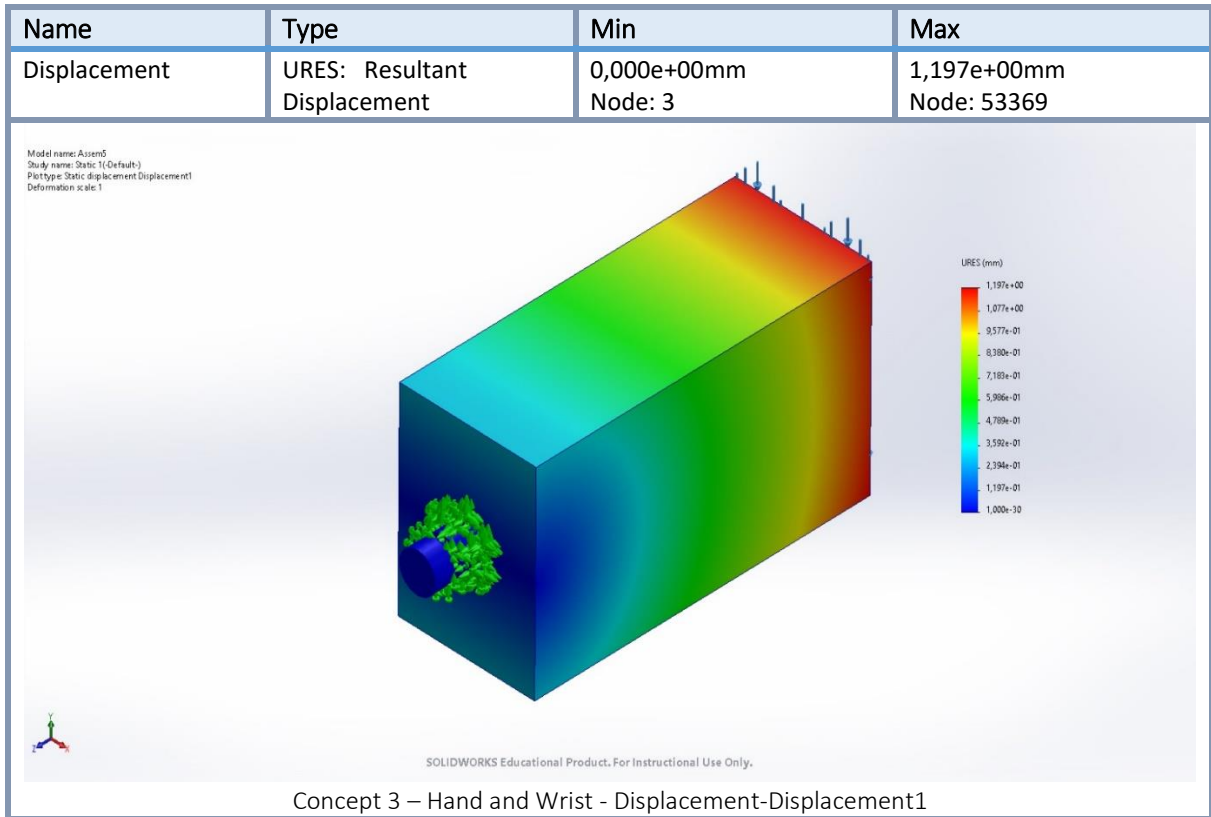
### Forearm





## Wrist





## Appendix H: Final Scoring Tables

### Functional scoring

		<i>Concepts</i>							
<b>Code</b>	<b>I</b>	<b>II</b>	<b>III</b>	<b>IV</b>	<b>V</b>	<b>VI</b>	<b>VII</b>	<b>Ideal</b>	
<i>Fu - As 2</i>	1	9	5	2	4	5	10	<b>12</b>	
<i>Fu - As 3</i>	8	14	11	2	10	10	16	<b>16</b>	
Total	9	23	16	4	14	15	26	<b>28</b>	
Percentage %	32.143	82.143	57.143	14.286	50.000	53.571	92.857	<b>100</b>	

### Fabrication scoring

		<i>Concepts</i>							
<b>Code</b>	<b>I</b>	<b>II</b>	<b>III</b>	<b>IV</b>	<b>V</b>	<b>VI</b>	<b>VII</b>	<b>Ideal</b>	
<i>Fa - Co 1</i>	5	7	6	2	2	4	8	<b>8</b>	
<i>Fa - Re 2</i>	9	11	10	6	9	9	12	<b>12</b>	
<i>Fa - We 1</i>	5	7	6	2	5	5	7	<b>8</b>	
<i>Fa - We 2</i>	2	2	2	2	3	2	4	<b>4</b>	
Total	21	27	24	12	19	20	31	<b>32</b>	
Percentage %	65.625	84.375	75	37.5	59.375	62.5	96.875	<b>100</b>	

### Overall scoring

		<i>Concepts</i>							
<b>Code</b>	<b>I</b>	<b>II</b>	<b>III</b>	<b>IV</b>	<b>V</b>	<b>VI</b>	<b>VII</b>	<b>Ideal</b>	
<i>Fu</i>	9	23	16	4	14	15	26	<b>28</b>	
<i>Fa</i>	21	27	24	12	19	20	31	<b>32</b>	
Total	30	50	40	16	33	35	57	<b>60</b>	
Percentage %	50	83.333	66.667	26.667	55	58.333	95	<b>100</b>	

Appendix I: FEA Simplified Wrist Adapter

Here is the threaded adapter in the threaded concept simplified by a cylinder to remove the small area in the transition from the adapter to the hand. Now the load is increased from 100N to 300N.

